

# Spin-identification of the Randall-Sundrum resonance in lepton-pair production at the LHC

P. Osland,<sup>a,1</sup> A. A. Pankov,<sup>b,2</sup> N. Paver<sup>c,3</sup> and A. V. Tsytin<sup>b,4</sup>

<sup>a</sup>Department of Physics and Technology, University of Bergen, Postboks 7803, N-5020  
Bergen, Norway

<sup>b</sup>The Abdus Salam ICTP Affiliated Centre, Technical University of Gomel, 246746  
Gomel, Belarus

<sup>c</sup>University of Trieste and INFN-Trieste Section, 34100 Trieste, Italy

## Abstract

The determination of the spin of the quantum states exchanged in the various non-standard interactions is a relevant aspect in the identification of the corresponding scenarios. We discuss the *identification* reach at LHC on the spin-2 of the lowest-lying Randall-Sundrum resonance, predicted by gravity with one warped extra dimension, against spin-1 and spin-0 non-standard exchanges with the same mass and producing the same number of events in the cross section. We focus on the angular distributions of leptons produced in the Drell-Yan process at the LHC, in particular we use as basic observable a “normalized” integrated angular asymmetry  $A_{CE}$ . Our finding is that the 95% C.L. *identification* reach on the spin-2 of the RS resonance (equivalently, the exclusion reach on both the spin-1 and spin-0 hypotheses for the peak) is up to a resonance mass scale of the order of 1.0 or 1.6 TeV in the case of weak coupling between graviton excitations and SM particles ( $k/\bar{M}_{Pl} = 0.01$ ) and 2.4 or 3.2 TeV for larger coupling constant ( $k/\bar{M}_{Pl} = 0.1$ ) for a time-integrated LHC luminosity of 10 or 100 fb<sup>-1</sup>, respectively. Also, some comments are given on the complementary rôles of the angular analysis and the eventual discovery of the predicted second graviton excitation in the identification of the RS scenario.

---

<sup>1</sup>E-mail: per.osland@ift.uib.no

<sup>2</sup>E-mail: pankov@ictp.it

<sup>3</sup>E-mail: nello.paver@ts.infn.it

<sup>4</sup>E-mail: tsytin@rambler.ru

# 1 Introduction

A common feature of the different New Physics (NP) scenarios that go beyond the Standard Model (SM) is the predicted existence of heavy new particles or “resonances”, that can be either produced or exchanged in reactions studied at high energy colliders. Such non-standard objects are expected to be in the TeV mass range, and could be revealed directly as peaks in the energy dependence of the measured cross sections.

For any model, given the expected statistics and experimental uncertainties, one can assess the corresponding *discovery* reach by determining the upper limit of the mass range where the resonance signal can be detected above the SM cross section to a given confidence level.

On the other hand, once a peak in the cross section is observed, further analysis is needed to distinguish the underlying non-standard dynamics against the other scenarios that potentially may cause a similar effect. In this regard, the expected *identification* reach is defined as the upper limit of the mass range where the model could be identified as the source of the peak or, equivalently, the other competitor models can be excluded for all values of their parameters. The determination of the spin of the resonance represents therefore an important selection among different classes of non-standard interactions.

Here, we consider the discrimination reach on the lowest-lying spin-2 Randall–Sundrum (RS) graviton resonance [1], that could be obtained from measurements of the Drell–Yan (DY) lepton-pair production processes ( $l = e, \mu$ ) at the LHC:

$$p + p \rightarrow l^+ l^- + X. \quad (1)$$

The determination of the spin-2 of the lowest-lying RS graviton resonance exchange against the spin-1 hypothesis in the context of experiments at LHC has recently been discussed, e.g., in Refs. [2–5], and some attention to the case of the spin-0 hypothesis has been given in Ref. [4]. Also, the exclusion of the spin-2 hypothesis against the spin-1 Stueckelberg  $Z'$  was discussed in Ref. [6]. An experimental search for spin-2, spin-1 and spin-0 new particles decaying to DY dilepton pairs has recently been performed at the Fermilab Tevatron  $p\bar{p}$  collider [7].

We would like to complement those analyses and assess the extent to which the domain in the RS parameters allowed by the discovery reach on the resonance is reduced by the request of simultaneous exclusion of *both* the hypotheses of spin-1 and spin-0 exchanges with the same mass, and mimicking the same peak in the dilepton invariant mass distribution (same number of events).

As is well known, the main tool to differentiate among the spin exchanges in the process (1) uses the different, and characteristic, dependencies on the angle  $\theta_{\text{cm}}$  between the incident quark or gluon and the final lepton in the dilepton center-of-mass frame. We shall base our discussion on the integrated center-edge asymmetry  $A_{\text{CE}}$ , that has the property of directly disentangling the spin-2 from vector interactions as illustrated in Refs. [8, 9]. This method represents an alternative to the use of the differential distributions  $dN/d\cos\theta_{\text{cm}}$ , where  $N$  represents the number of events.

We believe our analysis has sufficiently general features to be applicable also to the identification of other spin-2 exchange interactions, besides the RS model. We nevertheless prefer in the sequel to refer and expose in detail the procedure in the case of that mentioned scenario. Moreover, although strictly not necessary, we shall make comparisons with specific, “physically motivated” representative spin-0 and spin-1 models.

As an example of spin-0 contribution to the process (1), we can consider the sneutrino exchange envisaged by supersymmetric theories with  $R$ -parity breaking ( $\mathcal{R}_p$ ) [10,11]. In  $\mathcal{R}_p$  it is possible that some sparticles can be produced as  $s$ -channel resonances, thus appearing as peaks in the dilepton invariant mass distribution, if kinematically allowed.

Examples of competitor spin-1 mediated interactions, that can contribute to process (1) and show up as peaks in the cross section are, besides the SM  $\gamma$  and  $Z$ , the heavy  $Z'$  exchanges [12], and we will refer to those models for the comparison with the RS resonance exchange.

In Sec. 2 we discuss the LHC cross section and statistics for the production of a Randall–Sundrum heavy graviton. In Sec. 3 we identify the ranges in the number of events and mass that can originate from either the RS graviton or a spin-0 object, such as a sneutrino. This common range is referred to as the “signature space” of these models. A corresponding discussion is presented in Sec. 4 for the RS graviton and a spin-1 object, such as a  $Z'$ . In Sec. 5 we review the relevant angular distributions, and in Sec. 6 we show how these can be used to identify the RS graviton by means of the asymmetry  $A_{CE}$ . The results are collected in Sec. 7, where regions are identified in the plane spanned by the coupling strength  $c = k/\bar{M}_{Pl}$  and the mass  $M_R$ , where spin identification is possible. Finally, Sec. 8 presents some concluding remarks.

## 2 LHC cross sections and statistics for RS

Considering its great popularity in the context of models solving the gauge hierarchy problem, we here just recall that the simplest RS scenario is based on one compactified warped extra spatial dimension and two branes, such that the SM particles are confined to the so-called TeV brane while gravity can propagate in the whole 5-dimensional space. In this scenario TeV-scale, spin-2, narrow graviton resonances are predicted. The model depends on two independent parameters, that can be chosen as the dimensionless ratio  $c = k/\bar{M}_{Pl}$ , with  $k$  the 5-dimensional scalar curvature and  $\bar{M}_{Pl}$  the reduced 4-dimensional Planck scale ( $\bar{M}_{Pl} = M_{Pl}/\sqrt{8\pi}$ ), and  $m_1$ , the mass of the lowest-lying graviton resonance. The masses of the higher excitations  $G^{(n)}$  are given by  $m_n = m_1 x_n/x_1$ , where  $x_n$  are roots of the Bessel function  $J_1(x_n) = 0$  ( $x_1 = 3.8317$ ,  $x_2 = 7.0156$ ,  $x_3 = 10.1735$ ,...), and are therefore unevenly spaced. The mass pattern may therefore be distinctive of the model, if higher excitations in addition to the ground state would be discovered. A correlated parameter is represented by the physical scale on the TeV brane  $\Lambda_\pi = m_1/(c x_1)$ , whose inverse controls the strength of the graviton resonance coupling to standard matter. The (theoretically) natural ranges for these parameters are  $0.01 \leq c \leq 0.1$  and  $\Lambda_\pi < 10$  TeV [13]. Current discovery limits at 95% C.L. from the Fermilab Tevatron collider are for the first graviton mass: 300 GeV for  $c = 0.01$  and 900 GeV for  $c = 0.1$  [14].

### 2.1 Cross sections

In the SM, lepton pairs at hadron colliders can be produced at tree level via the following parton-level processes:

$$q\bar{q} \rightarrow \gamma, Z \rightarrow l^+l^-. \quad (2)$$

The first massive graviton mode  $G^{(1)}$  of the RS model, in the sequel denoted simply as  $G$  (and the mass  $m_1 \equiv M_G$ ), can be produced via quark–antiquark annihilation as well as

gluon–gluon fusion,

$$q\bar{q} \rightarrow G \rightarrow l^+l^- \quad \text{and} \quad gg \rightarrow G \rightarrow l^+l^-, \quad (3)$$

and can be observed as a peak in the dilepton invariant mass distribution. The inclusive differential cross section for  $G$  production and subsequent decay into lepton pairs at the LHC can be expressed as the sum:

$$\frac{d\sigma}{dM dy dz} = \frac{d\sigma_{q\bar{q}}}{dM dy dz} + \frac{d\sigma_{gg}}{dM dy dz}, \quad (4)$$

where  $M$  and  $y$  are invariant mass and rapidity of the lepton pairs, respectively, and  $z = \cos \theta_{\text{cm}}$  with  $\theta_{\text{cm}}$  the lepton-proton angle in the dilepton center-of-mass frame. Explicitly:

$$\begin{aligned} \frac{d\sigma_{q\bar{q}}}{dM dy dz} &= K \frac{2M}{s} \sum_q \left\{ [f_{q|P_1}(\xi_1, M) f_{\bar{q}|P_2}(\xi_2, M) + f_{\bar{q}|P_1}(\xi_1, M) f_{q|P_2}(\xi_2, M)] \frac{d\hat{\sigma}_{q\bar{q}}^{\text{even}}}{dz} \right. \\ &\quad \left. + [f_{q|P_1}(\xi_1, M) f_{\bar{q}|P_2}(\xi_2, M) - f_{\bar{q}|P_1}(\xi_1, M) f_{q|P_2}(\xi_2, M)] \frac{d\hat{\sigma}_{q\bar{q}}^{\text{odd}}}{dz} \right\}, \\ \frac{d\sigma_{gg}}{dM dy dz} &= K \frac{2M}{s} f_{g|P_1}(\xi_1, M) f_{g|P_2}(\xi_2, M) \frac{d\hat{\sigma}_{gg}}{dz}. \end{aligned} \quad (5)$$

Here,  $d\hat{\sigma}_{q\bar{q}}^{\text{even}}/dz$  and  $d\hat{\sigma}_{q\bar{q}}^{\text{odd}}/dz$  are the even and odd parts (under  $z \leftrightarrow -z$ ) of the partonic differential cross section  $d\hat{\sigma}_{q\bar{q}}/dz$ . Furthermore, the  $K$ -factor accounts for higher order QCD corrections and, at NLO, can be approximated by the well-known expression (see, for instance Ref. [15])

$$K = 1 + \frac{4}{3} \frac{\alpha_s}{2\pi} \left( 1 + \frac{4}{3} \pi^2 \right). \quad (6)$$

For simplicity, and to make our procedure more transparent, we shall use in the sequel a global, flat, factor  $K = 1.3$ . Although the full NLO corrections to the processes of interest here can require, as discussed in detail in Ref. [16], a somewhat larger  $K$ -factor, especially for gluon-initiated processes, this effect would tend to cancel in the  $A_{\text{CE}}$  asymmetry basic to our analysis, which is determined by ratios of angular-integrated (and mass-integrated around the resonance) cross sections. It may, however, have some bearing on the statistics, rendering the event rates based on the value 1.3 a slightly conservative estimate. Finally,  $f_{j|P_i}(\xi_i, M)$  are parton distribution functions in the protons  $P_1$  and  $P_2$ , and  $\xi_i$  are the parton fractional momenta:

$$\xi_1 = \frac{M}{\sqrt{s}} e^y, \quad \xi_2 = \frac{M}{\sqrt{s}} e^{-y}. \quad (7)$$

In deriving Eq. (5), the relations  $d\xi_1 d\xi_2 = (2M/s) dM dy$  and  $M^2 = \xi_1 \xi_2 s$  have been used, with  $s$  the  $pp$  C.M. energy squared. The minus sign in the odd term in that equation allows us to interpret the angle  $\theta_{\text{cm}}$  in the parton cross section as being relative to the quark or gluon momentum (rather than the proton momentum  $P_1$ ).

The lepton differential angular distribution, for dilepton invariant mass  $M$  in an interval of size  $\Delta M$  around the (narrow) resonance peak  $M_R$ , is defined by

$$\frac{d\sigma}{dz} = \int_{M_R - \Delta M/2}^{M_R + \Delta M/2} dM \int_{-Y}^Y \frac{d\sigma}{dM dy dz} dy, \quad (8)$$

with  $Y = \log(\sqrt{s}/M)$ .

The cross section for the narrow state production and subsequent decay into a DY pair,  $pp \rightarrow R \rightarrow l^+ l^-$ , is given by:

$$\sigma(R_{ll}) \equiv \sigma(pp \rightarrow R) \cdot \text{BR}(R \rightarrow l^+ l^-) = \int_{-z_{\text{cut}}}^{z_{\text{cut}}} dz \int_{M_R - \Delta M/2}^{M_R + \Delta M/2} dM \int_{-Y}^Y dy \frac{d\sigma}{dM dy dz}. \quad (9)$$

Actually, if angular cuts are imposed by detector acceptance,  $|z| \leq z_{\text{cut}}$ , then  $Y$  in Eqs. (8) and (9) must be replaced by some maximum value,  $y_{\text{max}} = y_{\text{max}}(z)$ .

One may notice that only terms in the partonic cross sections which are even in  $z$  contribute to the right-hand side of Eq. (8), because in the case of the proton-proton collider odd terms do not contribute after the integration over the rapidity  $y$ . This holds true for the SM  $\gamma$ - $Z$  interference term, as well as for SM- $G$  interference, with the SM partonic cross section being pure  $q\bar{q}$ -initiated at the considered order. Although such interference terms may appreciably contribute to the doubly-differential cross section  $d\sigma/dM dz$ , their contribution to the integral over  $M$  needed in Eqs. (8) and (9), symmetrical around the graviton resonance mass  $M_R$ , is negligibly small for  $M_Z \ll M_R$  and small resonance width (an approximation that will be assumed in the sequel), and negligible  $M$ -dependence of the overlap integral within the  $\Delta M$  bin. This fact is pointed out for the case of  $Z$ 's in, e.g., Refs. [6, 15], but also holds for the graviton resonance case. Thus, in Eqs. (8) and (9), we can just retain the SM and the  $G$  pole contributions.

Keeping  $z$ -symmetric terms only, the partonic cross sections relevant to the analysis presented below read [17, 18] (we follow the notation of [8]):

$$\left. \frac{d\hat{\sigma}_{q\bar{q}}^G}{dz} + \frac{d\hat{\sigma}_{gg}^G}{dz} \right|_{z \text{ even}} = \frac{\kappa^4 M^2}{640\pi^2} [\Delta_{q\bar{q}}(z) + \Delta_{gg}(z)] |\chi_G|^2, \quad (10)$$

$$\left. \frac{d\hat{\sigma}_{q\bar{q}}^{\text{SM}}}{dz} \right|_{z \text{ even}} = \frac{\pi\alpha_{\text{em}}^2}{6M^2} [S_q (1 + z^2)]. \quad (11)$$

In Eq. (10),  $\chi_G$  represents the graviton  $G$  propagator, with  $M_G$  and  $\Gamma_G$  the mass and total width, respectively:

$$\chi_G = \frac{M^2}{M^2 - M_G^2 + i M_G \Gamma_G}, \quad (12)$$

and, for the first massive mode,  $\kappa$  is given by [2, 19, 20]

$$\kappa = \sqrt{2} \frac{x_1}{M_G} c. \quad (13)$$

The total width can be written as  $\Gamma_G = \rho x_1^2 c^2 M_G$ , where  $\rho$  is a constant depending on the number of open decay channels. Assuming the graviton decays only to the SM particles, and with partial widths explicitly given in Refs. [2, 17, 19], one finds  $\Gamma_G = 1.43 c^2 M_G$ . With  $c \leq 0.1$  in the theoretically “natural” range, this value allows to use for the graviton resonance propagator the narrow-width approximation,

$$|\chi_G|^2 \rightarrow \delta(M - M_G) \frac{\pi M_G^2}{2\Gamma_G}. \quad (14)$$

The leading order angular dependencies in Eq. (10) are given by

$$\Delta_{q\bar{q}}(z) = \frac{\pi}{8N_C} \frac{5}{8} (1 - 3z^2 + 4z^4), \quad \Delta_{gg}(z) = \frac{\pi}{2(N_C^2 - 1)} \frac{5}{8} (1 - z^4), \quad (15)$$

where  $N_C$  is the number of quark colors.

For the SM partonic cross section of Eq. (11) one has, neglecting fermion masses:

$$S_q \equiv Q_q^2 Q_e^2 + 2Q_q Q_e v_q v_e \operatorname{Re} \chi_Z + (v_q^2 + a_q^2)(v_e^2 + a_e^2) |\chi_Z|^2, \quad (16)$$

where, for fermion  $f$ ,  $a_f = T_{3f}$ ,  $v_f = T_{3f} - 2Q_f \sin^2 \theta_W$ , and the  $Z$  propagator in the approximation  $M \gg M_Z$  is represented by

$$\chi_Z(M) \approx \frac{1}{\sin^2(2\theta_W)} \frac{M^2}{M^2 - M_Z^2}. \quad (17)$$

## 2.2 Statistical considerations

In the experimental discovery of a narrow resonance the observed width is determined by the dilepton invariant mass resolution, that we may associate to the size of the bin  $\Delta M$  introduced above. Clearly, on the one hand larger  $\Delta M$  would allow a larger chance of detecting the resonance and, on the other hand, for a narrow resonance falling within the bin the integral over  $\Delta M$  in Eq. (9) should be practically insensitive from the size of  $\Delta M$ . Conversely, such an integral should be essentially proportional to the size of  $\Delta M$  for the SM background. This background is dominated by the SM Drell-Yan process, other SM background contributions turn out to amount to at most a few percent of it [21].

Table 1: The number of signal events,  $N_S$ , in the RS model with  $c = 0.01$  including ATLAS detector cuts as a function of resonance mass  $M_G$  in a run of  $100 \text{ fb}^{-1}$  for the process  $pp \rightarrow e^+e^- + X$ ; the number of the SM background events,  $N_B$ , integrated over the bin and the minimum number of signal events  $N_S^{\min}$  required to detect the resonance (at  $5\sigma$ ).

$M_G$ (GeV)	Bin $\Delta M$ (GeV)	$N_S$	$N_B$	$N_S^{\min}$
1000	30.6	878.6	81.5	45.1
1500	42.9	108.9	14.6	19.1
1700	47.8	54.7	8.2	14.3
1800	50.2	39.6	6.2	12.5
1900	52.6	29.0	4.8	10.9
2000	55.0	21.4	3.7	10.0
2100	57.4	16.0	2.9	10.0
2200	59.8	12.1	2.2	10.0
2300	62.3	9.2	1.8	10.0
2400	64.7	7.0	1.4	10.0
2500	67.1	5.4	1.1	10.0

Regarding the bin size, it depends on the energy resolution. For the ATLAS detector, the bin size  $\Delta M$  at invariant dilepton mass  $M$  measured in TeV units, can be parameterized as [22]:

$$\Delta M = 24 (0.625M + M^2 + 0.0056)^{1/2} \text{ GeV}. \quad (18)$$

For  $M > 3 \text{ TeV}$ , the  $M^2$  term dominates in Eq. (18) and the bin size grows linearly in  $M$ , so that  $\Delta M \sim 24M \text{ GeV}$  for large  $M$ . Similar results, comparable to about 10%, hold for the CMS detector [23]. Throughout the paper we will use Eq. (18) for the bin size.

At the LHC, with integrated luminosity  $\mathcal{L}_{\text{int}} = 100 \text{ fb}^{-1}$ , the number of signal (resonant) events can be computed by using  $N_S = \sigma(R_{ll}) \epsilon_l \mathcal{L}_{\text{int}}$  and the background events are defined as  $N_B = N_{SM}$  (background integrated over the bin). Here,  $\epsilon_l$  is the experimental reconstruction efficiency, taken to be 0.9 both for electrons and muons. To compute cross sections we use the CTEQ6 parton distributions [24]. We impose angular cuts relevant to the LHC detectors. The lepton pseudorapidity cut is  $|\eta| < \eta_{\text{cut}} = 2.5$  for both leptons (this leads to a boost-dependent cut on  $z$  [8]), and in addition to the angular cuts, we impose on each lepton a transverse momentum cut  $p_{\perp} > p_{\perp}^{\text{cut}} = 20 \text{ GeV}$ . Analogous to previous references, in the analysis given here, we have adopted the criterion for the discovery limit that  $5\sqrt{N_B}$  events or 10 events, whichever is larger, constitutes a signal. The number of DY background events ( $N_B$ ) inside each bin, the minimum number of signal events required to detect a graviton resonance ( $N_S^{\text{min}}$ ) and the resonant signal events ( $N_S$ ) at various  $M_G$  are summarized in Table 1. Only electron pairs are included in Table 1.

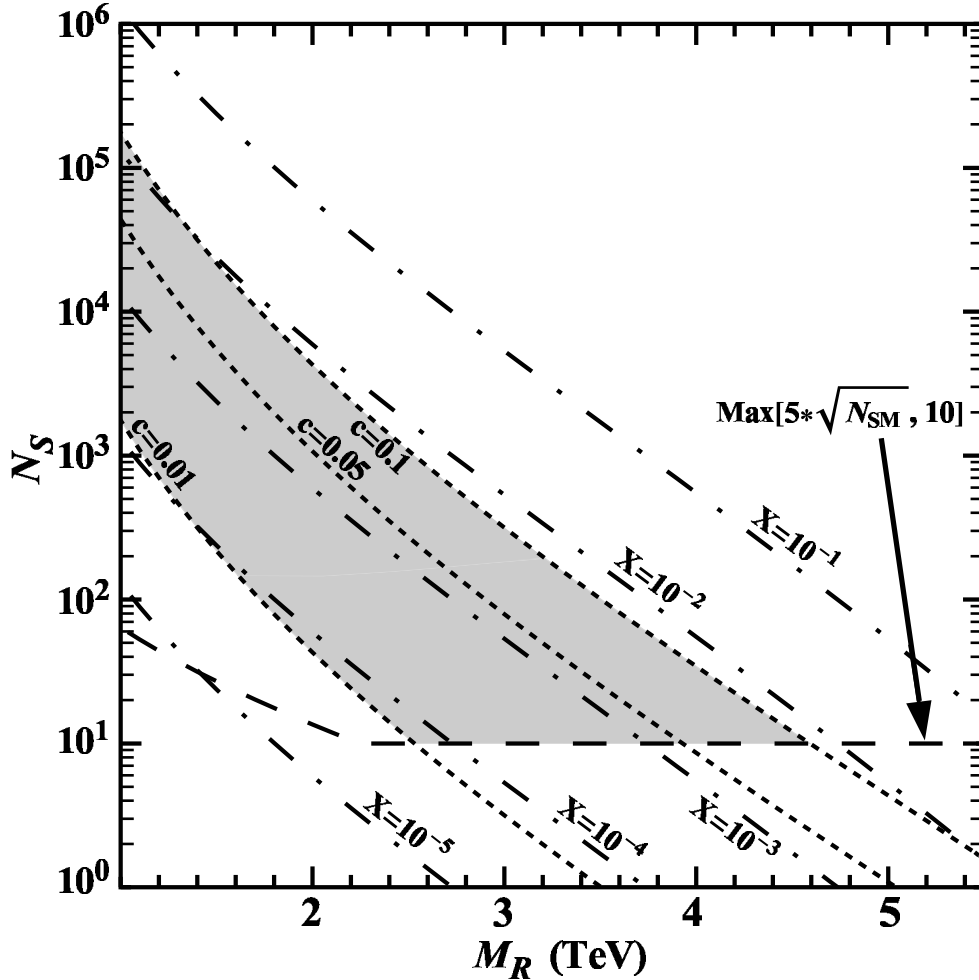


Figure 1: Expected number of resonance (signal) events  $N_S$  vs.  $M_R$  ( $R = G, \tilde{\nu}_\tau$ ) at  $\mathcal{L}_{\text{int}} = 100 \text{ fb}^{-1}$  for graviton and sneutrino resonant production with values of  $c = 0.01, 0.05, 0.1$  (short dashed curves) and  $X$  (see Eq. (24)) ranging from  $10^{-5}$  to  $10^{-1}$  in steps of 10 (dash-dotted curves) and the minimum number of signal events (dashed curve) needed to detect the resonance above the background in the process  $pp \rightarrow l^+l^- + X$  ( $l = e, \mu$ ). Shaded area corresponds to potential overlap of graviton signature space with that for sneutrino resonant production.

Fig. 1 shows the expected number of resonant (signal) events  $N_S$  *vs.* resonance mass  $M_R$  ( $R = G$ ) at  $\mathcal{L}_{\text{int}} = 100 \text{ fb}^{-1}$  for graviton production with values of  $c = 0.01, 0.05, 0.1$  (dashed curves), and the minimum number of signal events needed to detect it above the background. With the assumption of efficiencies as stated above one finds that, with  $100 \text{ fb}^{-1}$  of integrated luminosity, one can explore a massive graviton up to a mass of about 2.5 TeV with  $c = 0.01$  ( $5\sigma$  level), and this limit can be pushed to  $\approx 4.5 \text{ TeV}$  with  $c = 0.1$ , consistent with the results of [13]. While the analysis above is for the specific RS model, the general features of this analysis may hold for a wider class of models which support narrow resonances and predict spin-2 intermediate states. We shall refer to a region in the space spanned by resonance mass and number of events, that can be populated by a certain model, as the “signature space” of that model. We now proceed to sketch the competing (with the spin-2 resonance) non-standard spin-0 and spin-1 interactions, and their respective signature spaces.

### 3 Signature spaces of RS $G$ and sneutrino in $R_p$

As mentioned in Sec. 1, models based on  $R_p$  SUSY can mimic the RS graviton in a certain part of the parameter space as far as the mass and narrowness of the resonance is concerned. At tree-level, the relevant parton process for DY lepton-pair production is in  $R$ -parity breaking given by spin-0 sneutrino ( $\tilde{\nu}$ ) formation from quark-antiquark annihilation and subsequent leptonic decay:

$$q\bar{q} \rightarrow \gamma, Z, \tilde{\nu} \rightarrow l^+ l^-. \quad (19)$$

The corresponding partonic cross section is given by [10]

$$\frac{d\hat{\sigma}_{q\bar{q}}}{dz} = \frac{d\hat{\sigma}_{q\bar{q}}^{\text{SM}}}{dz} + \frac{d\hat{\sigma}_{q\bar{q}}^{\tilde{\nu}}}{dz}, \quad (20)$$

where the pure resonant term reads

$$\frac{d\hat{\sigma}_{q\bar{q}}^{\tilde{\nu}}}{dz} = \frac{1}{3} \frac{\pi \alpha_{\text{em}}^2}{4 M^2} \left( \frac{\lambda \lambda'}{e^2} \right)^2 |\chi_{\tilde{\nu}}|^2 \delta_{qd}. \quad (21)$$

Here, the propagator of the sneutrino  $\chi_{\tilde{\nu}}$  is represented by

$$\chi_{\tilde{\nu}} = \frac{M^2}{M^2 - M_{\tilde{\nu}}^2 + i M_{\tilde{\nu}} \Gamma_{\tilde{\nu}}}, \quad (22)$$

$M_{\tilde{\nu}}$  ( $\Gamma_{\tilde{\nu}}$ ) is the mass (total decay width) of the sneutrino,  $\lambda'$  and  $\lambda$  are the relevant  $R$ -parity-violating couplings of  $d\bar{d}$  and  $l^+ l^-$  to the sneutrino, respectively. We note that the process (19), where the intermediate state is a sneutrino, requires *two*  $R$ -parity-violating couplings to be non-zero.<sup>1</sup> For the present case, the  $K$ -factor has been studied for a range of sneutrino masses, and for different parton distribution functions [26]. The value adopted for the graviton case,  $K = 1.3$ , remains a good approximation.

---

<sup>1</sup>A different scenario was investigated in [25], where only *one* such coupling was assumed non-zero. Then a squark would be exchanged in the  $t$ - or  $u$ -channel, and the angular distribution would be rather different.



In the narrow width approximation the  $\tilde{\nu}$ -exchange cross section (21) can be written as:

$$\frac{d\hat{\sigma}_{q\bar{q}}^{\tilde{\nu}}}{dz} \approx \frac{\pi}{24} \frac{X}{M_{\tilde{\nu}}} \delta(M - M_{\tilde{\nu}}) \delta_{qd}, \quad (23)$$

where

$$X = (\lambda')^2 B_l. \quad (24)$$

Here  $B_l$  is the sneutrino leptonic branching ratio and  $\lambda'$  the relevant coupling to the  $d\bar{d}$  quarks. Indeed, due to  $SU(2)$  invariance, the sneutrino, which is a  $T_3 = +\frac{1}{2}$ -member of the doublet, can only couple to a *down*-type quark. This model depends therefore on two independent parameters, i.e., the sneutrino mass  $M_{\tilde{\nu}}$  and  $X$ . With  $i, j, k$  generation indices, the  $R$ -parity-violating coupling of interest is  $\lambda'_{ijk} = \lambda'_{i11}$ , with  $i$  denoting the sneutrino generation. Among these,  $\lambda'_{111}$  is rather constrained, whereas  $\lambda'_{211}$  and  $\lambda'_{311}$  could be as large as  $10^{-1}$ – $10^{-2}$  for a 100 GeV sneutrino, and larger for a heavier one [27].

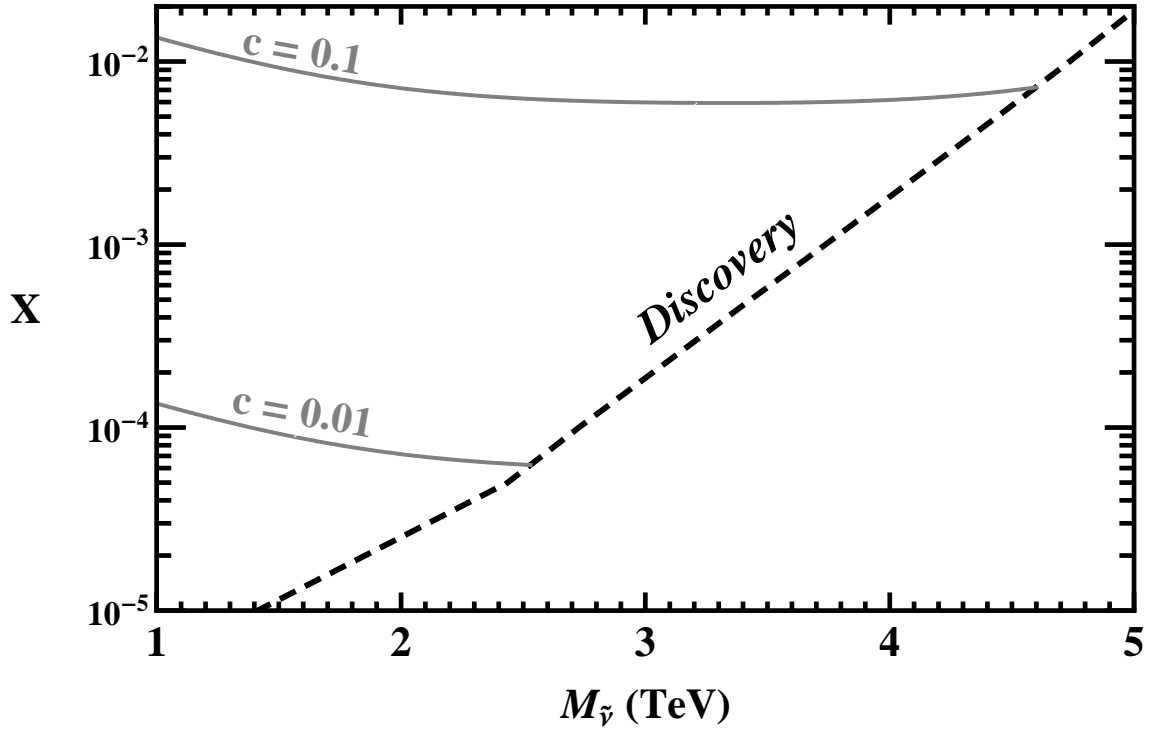


Figure 2: The discovery reach at the  $5\sigma$  level in the plane  $(M_{\tilde{\nu}}, X)$  obtained from lepton pair production ( $l = e, \mu$ ) at the LHC with  $\mathcal{L}_{\text{int}} = 100 \text{ fb}^{-1}$ . The discovery limit is defined by  $5\sqrt{N_{SM}}$  or by 10 events, whichever is larger. The kink in the plot is the point of transition between the two criteria. Indicated is the domain in sneutrino parameters for discovery in the reach of LHC. The area enclosed between the two solid lines and the dashed line corresponds to the shaded area shown in Fig. 1.

Quantitatively, the current constraints on  $X$  are rather loose. The number of signal events as a function of the spin-0 mass for the case of sneutrino production with values of  $X$  ranging from  $10^{-5}$  to  $10^{-1}$  in steps of 10 (dash-dotted curves), are given in Fig. 1. The calculation has been performed under the assumptions and kinematical cuts exposed in Sec. 2.2. From Fig. 1 one can easily obtain the discovery reach on sneutrino parameters

( $5\sigma$  level) and translate them into the plane  $(M_{\tilde{\nu}}, X)$  exhibited in Fig. 2. In this figure, the discovery region is on the left of the dashed line, and the gray ( $\sim$  horizontal) lines limit the “confusion” domain with the RS graviton in event rates, with  $c = 0.01$  and  $c = 0.1$ , respectively, see also Ref. [11].

In Fig. 1, the shaded area indicates the overlap of the LHC-discovery parameter space for the  $R_p$  scenario *via*  $\sigma(pp \rightarrow \tilde{\nu} \rightarrow l^+ l^-)$  and that of the lowest RS graviton scenario *via*  $\sigma(pp \rightarrow G \rightarrow l^+ l^-)$ . The figure indicates that, as far as the total production cross section of DY dilepton pairs is concerned, there exists a significantly extended domain in the  $(M_{\tilde{\nu}}, X)$  plane where sneutrino  $\tilde{\nu}$  production can mimic RS graviton  $G$  formation in its theoretically “natural” domain  $(M_G, c)$ : in these respective domains, the two scenarios can lead to the same number of events under the resonance peak,  $N_S(G \rightarrow l^+ l^-) = N_S(\tilde{\nu} \rightarrow l^+ l^-)$ . In other words, the two models are indistinguishable in the overlapping domains of their parameter spaces, indicated by the shaded area in Fig. 1. Clearly, outside the “common” shaded area, the two scenarios might be differentiated by means of event rates. For the identification, the two models must be discriminated in the “confusion” region in Fig. 1, this can be done by the spin determination of the RS resonance.

## 4 Signature spaces of RS $G$ and $Z'$

Turning now to spin-1 resonance exchange, the differential cross section for the relevant partonic process  $q\bar{q} \rightarrow \gamma, Z, Z' \rightarrow l^+ l^-$  reads at leading order

$$\frac{d\hat{\sigma}_{q\bar{q}}}{dz} = \frac{d\hat{\sigma}_{q\bar{q}}^{\text{SM}}}{dz} + \frac{d\hat{\sigma}_{q\bar{q}}^{Z'}}{dz}, \quad (25)$$

with

$$\left. \frac{d\hat{\sigma}_{q\bar{q}}^{Z'}}{dz} \right|_{z=\text{even}} = \frac{\pi \alpha_{\text{em}}^2}{6M^2} [S'_q (1 + z^2)], \quad (26)$$

and, neglecting fermion masses:

$$S_q^{Z'} \equiv (v_q'^2 + a_q'^2)(v_e'^2 + a_e'^2) |\chi_{Z'}|^2. \quad (27)$$

Here, we have introduced the  $Z'$  vector and axial-vector couplings to SM fermions, and the  $Z'$  propagator  $\chi_{Z'}$  is represented by

$$\chi_{Z'} = \frac{M^2}{M^2 - M_{Z'}^2 + i M_{Z'} \Gamma_{Z'}}. \quad (28)$$

According to previous arguments, in the sequel we neglect  $(\gamma, Z) - Z'$  interference terms in the cross section. Moreover, effects from a potential  $Z - Z'$  mixing are also disregarded.

As anticipated in Sec. 1, in addition to a generic spin-1 exchange, we will consider the discrimination reach on the spin-2 lowest RS resonance from the, rather popular and physically motivated,  $Z'$  scenarios where the couplings in Eq. (27) are constrained to have fixed values. One such model is the so-called sequential model (SSM), where the  $Z'$  couplings to fermions are the same as those of the SM  $Z$ .

Furthermore, we will consider: (i) the three possible  $U(1)$   $Z'$  scenarios originating from the exceptional group  $E_6$  breaking; and (ii) the  $Z'$  predicted by a left-right symmetric model that can originate from an  $SO(10)$  GUT. While detailed descriptions of these models can

be found, e. g., in Ref. [12], we just recall that the three heavy neutral gauge bosons are denoted by  $Z'_\chi$ ,  $Z'_\psi$  and  $Z'_\eta$  with specific coupling constants to SM matter displayed in Table 2. Regarding the case (ii), the mentioned left-right (LR) model predicts a heavy neutral gauge boson  $Z'_{LR}$  generally coupled to a linear combination of the right-handed and  $B$ - $L$  currents [ $B$  and  $L$  are baryon and lepton numbers, respectively]:

$$J_{LR}^\mu = \alpha_{LR} J_{3R}^\mu - (1/2\alpha_{LR}) J_{B-L}^\mu \quad \text{with } \alpha_{LR} = \sqrt{(c_W^2 g_R^2 / s_W^2 g_L^2) - 1}. \quad (29)$$

Here,  $g_L = e/s_W$  and  $g_R$  are the  $SU(2)_L$  and  $SU(2)_R$  coupling constants with  $s_W^2 = 1 - c_W^2 \equiv \sin^2 \theta_W$ ; the parameter  $\alpha_{LR}$  is restricted to the range  $\sqrt{2/3} \lesssim \alpha_{LR} \lesssim \sqrt{2}$ . The upper bound corresponds to the so-called LR-symmetric  $Z'_{LR}$  model with  $g'_R = g'_L$ , while the lower bound is found to coincide with the  $Z'_\chi$  model introduced above.

Finally, we will include in our analysis the case of the  $Z'_{ALR}$  predicted by the so-called “alternative” left-right scenario [12, 28].

All numerical values of the  $Z'$  couplings needed in Eq. (27) are collected in Table 2, where:  $v'_f(a'_f) = (g_L^{f'} \pm g_R^{f'})/2$ ;  $A = \cos \beta / 2\sqrt{6}$ ,  $B = \sqrt{10} \sin \beta / 12$  with  $\beta = 0, \pi/2$  and  $\arctan(-\sqrt{5/3})$  for the  $Z'_\chi$ ,  $Z'_\psi$  and  $Z'_\eta$ , respectively. We have introduced the notations  $g_{Z'} = 1/c_W$  for the  $E_6$  and the LR models and  $g_{Z'} = 1/(s_W c_W \sqrt{1 - 2s_W^2})$  for the ALR model. Current direct search limits on  $Z'$  masses from the Fermilab Tevatron are of the order of 900 GeV or less [29].

Table 2: Left-handed and right-handed couplings of the first generation of SM fermions to the  $Z'$  gauge bosons, needed in Eq. (27).

$E_6$ model				
fermions ( $f$ )	$\nu$	$e$	$u$	$d$
$g_L^{f'}/g_{Z'}$	$3A + B$	$3A + B$	$-A + B$	$-A + B$
$g_R^{f'}/g_{Z'}$	0	$A - B$	$A - B$	$-3A - B$
Left-Right model (LR)				
$g_L^{f'}/g_{Z'}$	$\frac{1}{2\alpha_{LR}}$	$\frac{1}{2\alpha_{LR}}$	$-\frac{1}{6\alpha_{LR}}$	$-\frac{1}{6\alpha_{LR}}$
$g_R^{f'}/g_{Z'}$	0	$\frac{1}{2\alpha_{LR}} - \frac{\alpha_{LR}}{2}$	$-\frac{1}{6\alpha_{LR}} + \frac{\alpha_{LR}}{2}$	$-\frac{1}{6\alpha_{LR}} - \frac{\alpha_{LR}}{2}$
Alternative Left-Right model (ALR)				
$g_L^{f'}/g_{Z'}$	$-\frac{1}{2} + s_W^2$	$-\frac{1}{2} + s_W^2$	$-\frac{1}{6}s_W^2$	$-\frac{1}{6}s_W^2$
$g_R^{f'}/g_{Z'}$	0	$-\frac{1}{2} + \frac{3}{2}s_W^2$	$\frac{1}{2} - \frac{7}{6}s_W^2$	$\frac{1}{3}s_W^2$

The  $Z'$  partial decay widths into massless fermion-antifermion pairs in  $E_6$  and LR models are functions of  $\beta$  and  $\alpha_{LR}$ , respectively. From the analysis of Refs. [12, 30] it turns out that, in the absence of “exotic” decay channels, the total width  $\Gamma_{Z'} \ll M_{Z'}$ , so that the narrow width approximation to the  $Z'$  propagator should be adequate for our numerical estimates.

The number of  $Z'$  signal events as a function of resonance mass for the representative models summarized in Table 2, and LHC luminosity of  $100 \text{ fb}^{-1}$ , are given in Fig. 3. From this figure, one can easily obtain the  $5\sigma$  level discovery reaches on the corresponding  $Z'$

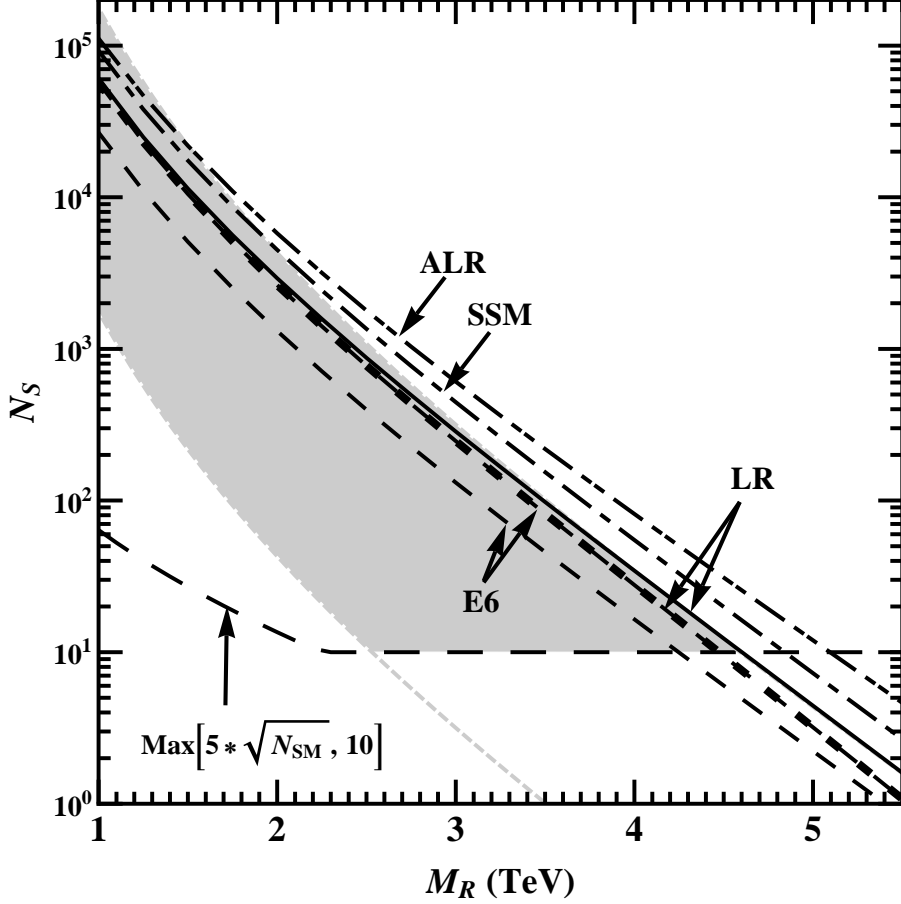


Figure 3: Same as in Fig. 1 but for number of resonance events  $N_S$  vs.  $M_R$  ( $R = G, Z'$ ) for graviton and  $Z'$  resonant production and the minimum number of signal events needed to detect the resonances above the background in the process  $pp \rightarrow l^+l^- + X$  ( $l = e, \mu$ ). The two “LR” lines refer to the extreme values for  $\alpha_{LR}$ . The shaded area is the overlap of graviton and sneutrino signature spaces for  $0.01 < c < 0.1$ , with  $\mathcal{L}_{\text{int}} = 100 \text{ fb}^{-1}$ .

masses, presented as a histogram in Fig. 4. These estimates are numerically consistent with those in Refs. [6, 12] and [28, 31–35].

In these cases, the  $Z'$  signature spaces reduce to lines, and Fig. 3 shows that, at the assumed LHC luminosity, the lowest, RS spin-2, resonance can be discriminated against the ALR and SSM spin-1  $Z'$  scenarios already at the level of event rates in a large range of  $M_{Z'}$  values, with no need for further analyses based on angular distributions. Only the  $E_6$  and LR  $Z'$  models possess a “confusion region” with the RS resonance  $G$ , concentrated near the upper border of the graviton allowed signature domain. This may represent an interesting information by itself.

In the next sections, we turn to the identification of the spin-2 of the first RS resonance, *vs.* the spin-1 and spin-0 hypotheses.

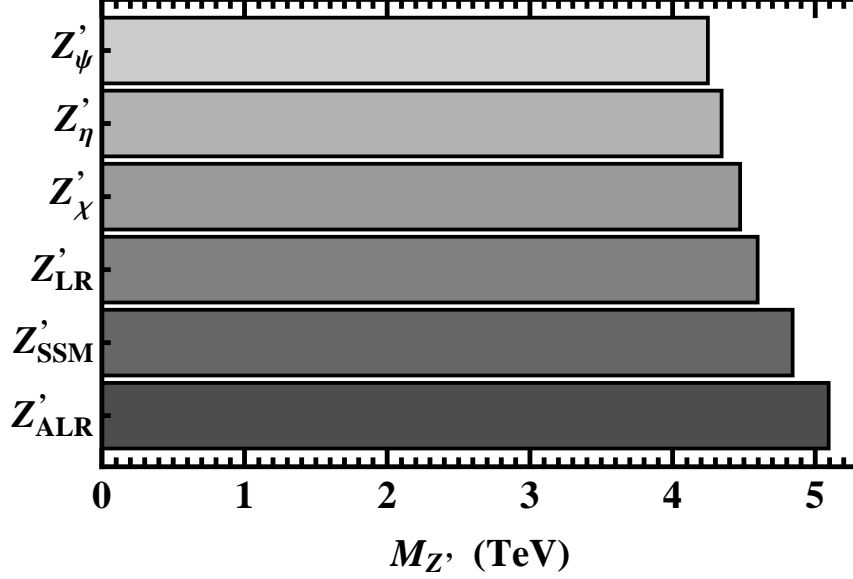


Figure 4: Discovery limits at the  $5\sigma$  level for neutral gauge bosons of representative models, obtained from lepton pair production ( $l = e, \mu$ ) at the LHC with  $\mathcal{L}_{\text{int}} = 100 \text{ fb}^{-1}$ .

## 5 Angular distributions in the dilepton channel

The normalized angular distributions of the relevant parton processes, mediated by spin-2, spin-1 and spin-0 formation and subsequent decay to DY pairs, are shown in Table 3, as summarized, e.g., also in Refs. [3, 4].

For simplicity, and according to the considerations made in Sec. 2, in this table only the  $z$ -even terms in the parton differential cross sections are retained,  $z$ -odd contributions disappear from the observables we will consider.

The correspondence between spin and angular distribution is quite sharp: a spin-0 resonance determines a flat angular distribution, spin-1 corresponds to a parabolic shape, and spin-2 yields a quartic distribution. The CDF collaboration has recently attempted angular distribution analyses using the cumulative DY data at the  $p\bar{p}$  Tevatron collider, their results are reported in Ref. [7]. The LHC promises tests of the spin hypotheses with significantly higher sensitivity, due to the definitely higher statistics allowed by the foreseen larger energy and luminosity.

Using Eq. (8), one can derive the angular distributions determined by spin-2 RS graviton resonance, spin-1  $V$  and spin-0  $S$ , respectively. These distributions can be conveniently written in a self-explanatory way as [ $G$  denotes the spin-2 resonance, while  $V$  and  $S$  denote the spin-1 and spin-0 cases, respectively]:

$$\frac{d\sigma(G_u)}{dz} = \frac{3}{8} (1 + z^2) \sigma_{q\bar{q}}^{\text{SM}} + \frac{5}{8} (1 - 3z^2 + 4z^4) \sigma_{q\bar{q}}^G + \frac{5}{8} (1 - z^4) \sigma_{g\bar{g}}^G, \quad (30)$$

$$\frac{d\sigma(V_u)}{dz} = \frac{3}{8} (1 + z^2) (\sigma_{q\bar{q}}^{\text{SM}} + \sigma_{q\bar{q}}^V), \quad (31)$$

$$\frac{d\sigma(S_u)}{dz} = \frac{3}{8} (1 + z^2) \sigma_{q\bar{q}}^{\text{SM}} + \frac{1}{2} \sigma_{q\bar{q}}^S. \quad (32)$$

Table 3: Normalized angular distributions for the decay products of spin-0, spin-1 and spin-2 resonances, considering only even terms in  $z \equiv \cos \theta_{\text{cm}}$  for parton subprocesses.

Process	Normalized density for $\cos \theta_{\text{cm}}$ , $(1/\hat{\sigma})d\hat{\sigma}/dz$
$q\bar{q} \rightarrow (\gamma, Z) \rightarrow l^+l^-$ $q\bar{q} \rightarrow Z' \rightarrow l^+l^-$	$\frac{3}{8}(1+z^2)$
$gg \rightarrow G \rightarrow l^+l^-$	$\frac{5}{8}(1-z^4)$
$q\bar{q} \rightarrow G \rightarrow l^+l^-$	$\frac{5}{8}(1-3z^2+4z^4)$
$\bar{q}q \rightarrow \tilde{\nu} \rightarrow l^+l^-$	$\frac{1}{2} \text{ (flat)}$

Corresponding to Eqs. (30)–(32), the integrated  $pp$  production cross sections for the  $G$ ,  $V$  and  $S$  hypotheses are given by

$$\sigma(G_{ll}) = \sigma_{q\bar{q}}^{\text{SM}} + \sigma_{q\bar{q}}^G + \sigma_{gg}^G, \quad \sigma(V_{ll}) = \sigma_{q\bar{q}}^{\text{SM}} + \sigma_{q\bar{q}}^V, \quad \sigma(S_{ll}) = \sigma_{q\bar{q}}^{\text{SM}} + \sigma_{q\bar{q}}^S. \quad (33)$$

Detector cuts are not taken into account in the above Eqs. (30)–(33). We shall use these relations for illustration purposes, in order to better expose the most important features of the method we use. The final numerical results, as well as the relevant figures that will be presented in the sequel refer to the full calculation, with detector cuts taken into account. It turns out, however, that such results are numerically close to those derived from the application of Eqs. (30)–(33).

The angular distributions arising from the spin-2, spin-1 and spin-0 resonances are represented in Fig. 5, for the same peak masses  $M_R$  in the three hypotheses and the same number of signal events,  $N_S$ , under the peak. The angular distributions in this figure are somewhat distorted compared to those in Table 3, because of (i) the smearing due to the parton distributions in the protons, (ii) different partons contribute with different weight to the different channels, and (iii) detector cuts are taken into account.

## 6 Identification of the spin-2 of the RS graviton

### 6.1 Center-edge asymmetry

To assess the identification power of the LHC of distinguishing the spin-2 RS resonance from both spin-1 and spin-0 exchanges, we adopt the integrated center-edge asymmetry  $A_{\text{CE}}$  introduced in Refs. [8, 9]. Basically, the advantage of this observable lies in its insensitivity to spin-1 exchanges in the  $s$ -channel. This property follows from the fact that such exchanges are characterized by the same  $z$ -distributions as the SM  $\gamma$ - and  $Z$ -exchanges, see Eq. (31). Thus, deviations of  $A_{\text{CE}}$  from the SM predictions could be attributed to graviton exchanges and, accordingly, one could expect a particularly high sensitivity in the identifi-

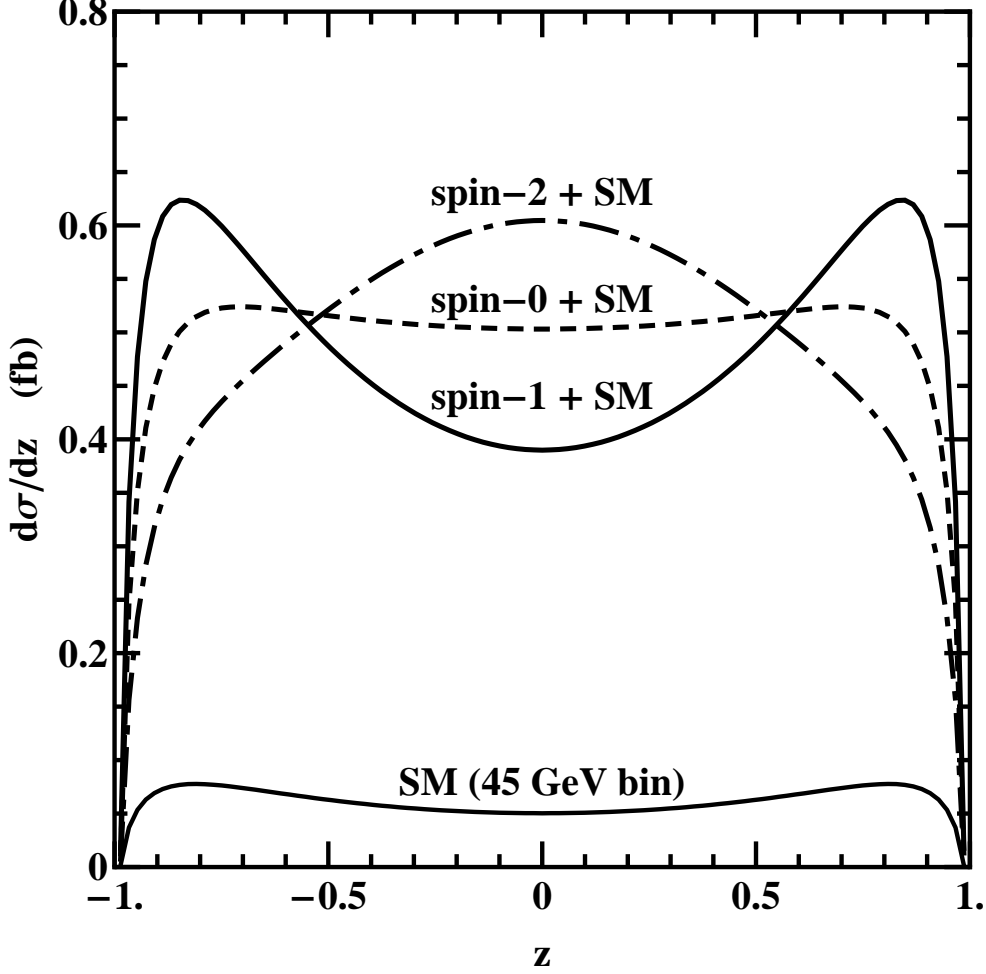


Figure 5: Angular distribution of leptons in the dilepton center of mass system for (i) spin-2 graviton resonant production,  $d\sigma(pp \rightarrow G \rightarrow l^+l^-)/dz$ , in the RS model with  $c=0.01$ ; (ii) spin-0 resonant production,  $d\sigma(pp \rightarrow S \rightarrow l^+l^-)/dz$ ; (iii) spin-1 resonant production,  $d\sigma(pp \rightarrow V \rightarrow l^+l^-)/dz$ . We take  $M_R = 1.6$  TeV and assume equal numbers of resonant DY events.

cation of this kind of effects. Also, being “normalized” to the cross section integrated over angles, one may hope this observable to be less sensitive to systematic uncertainties.

In the present application, we define the center-edge asymmetry, with  $R$  labelling the three hypotheses we want to compare, as:

$$A_{\text{CE}}(M_R) = \frac{\sigma_{\text{CE}}(R_{ll})}{\sigma(R_{ll})}, \quad (34)$$

with the “center minus edge” cross section:

$$\sigma_{\text{CE}} \equiv \left[ \int_{-z^*}^{z^*} - \left( \int_{-z_{\text{cut}}}^{-z^*} + \int_{z^*}^{z_{\text{cut}}} \right) \right] \frac{d\sigma(R_{ll})}{dz} dz. \quad (35)$$

Here:  $0 < z^* < z_{\text{cut}}$  is a, a priori free, value of  $\cos \theta_{\text{cm}}$  that defines the separation between the “center” and the “edge” angular regions; in the approximation  $z_{\text{cut}} = 1$ ,  $d\sigma(R_{ll})/dz$  are given by Eqs. (30)–(32) and the total cross sections  $\sigma(R_{ll})$  by Eq. (33).

We assume that a deviation from the SM is discovered in the cross section for dilepton production at LHC in the form of a narrow peak in the dilepton invariant mass, and attempt the determination of the domain in the RS parameter space where such a peak can be *identified* as being caused by the spin-2 RS exchange, and the spin-0 and spin-1 hypotheses excluded. We also assume the integrated center-edge asymmetry evaluated within the RS model to be consistent with the measured data, and call this spin-2 model the “true” or “best-fit” model. We want to assess the level at which this “true” model is distinguishable from the other hypotheses, with spin-0 and spin-1, that can compete with it as sources of a resonance peak in dilepton production yielding in particular the same number of signal events.

The explicit  $z^*$ -dependence of the center-edge asymmetries for the three cases of interest here, obtained from Eqs. (30)–(33) and Eqs. (34)–(35) are, in the same notations:

$$A_{\text{CE}}^G = \epsilon_q^{\text{SM}} A_{\text{CE}}^V + \epsilon_q^G \left[ 2z^{*5} + \frac{5}{2}z^*(1 - z^{*2}) - 1 \right] + \epsilon_g^G \left[ \frac{1}{2}z^*(5 - z^{*4}) - 1 \right], \quad (36)$$

$$A_{\text{CE}}^V \equiv A_{\text{CE}}^{\text{SM}} = \frac{1}{2}z^*(z^{*2} + 3) - 1, \quad (37)$$

$$A_{\text{CE}}^S = \epsilon_q^{\text{SM}} A_{\text{CE}}^V + \epsilon_q^S (2z^* - 1). \quad (38)$$

Here,  $\epsilon_q^G$ ,  $\epsilon_g^G$ s and  $\epsilon_q^{\text{SM}}$  are the fractions of resonant events for  $q\bar{q}, gg \rightarrow G \rightarrow l^+l^-$  and SM background, respectively, with  $\epsilon_q^G + \epsilon_g^G + \epsilon_q^{\text{SM}} = 1$ . They are determined by the ratios of  $\sigma_{q\bar{q}}^G$ , etc., of Eq. (30) and  $\sigma(G_{ll})$  of Eq. (33), and shown in Fig. 6 for two values of  $c$ .

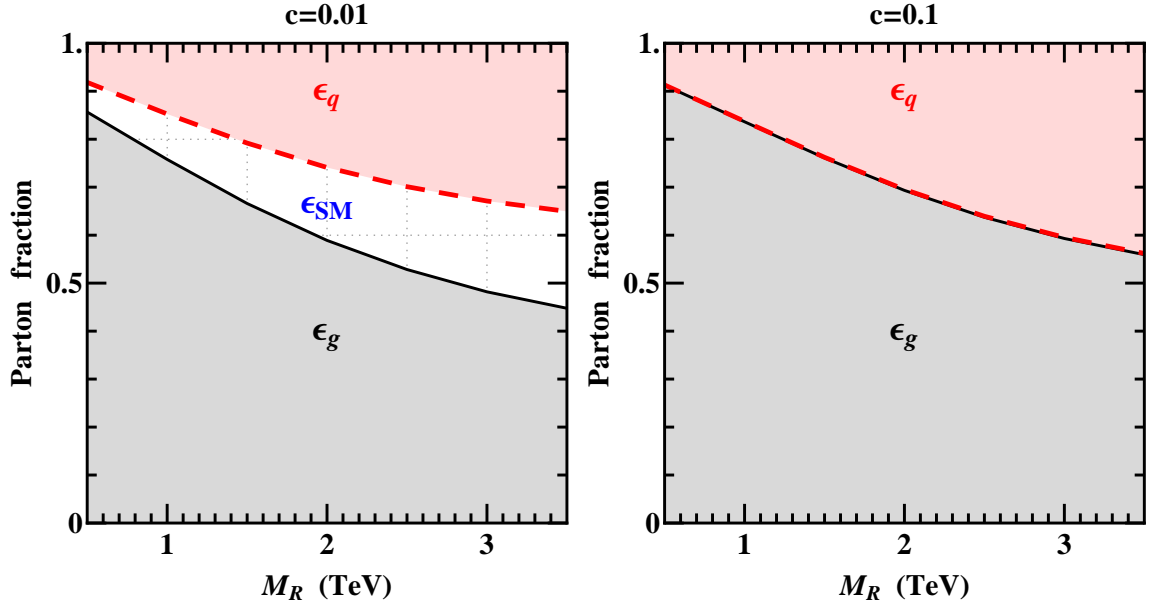


Figure 6: Contribution of gluon-gluon fusion  $\epsilon_g^G$  and quark-antiquark annihilation  $\epsilon_q^G$  to graviton production at the LHC as a function of mass, displayed cumulatively, for  $c = 0.01$  and  $0.1$ .

Analogous definitions hold for the other cases. One should emphasize again that, for spin-1,  $A_{\text{CE}}^V$  and the SM background (predominantly from the DY continuum [4]) have the same form, independent of couplings and resonance mass.



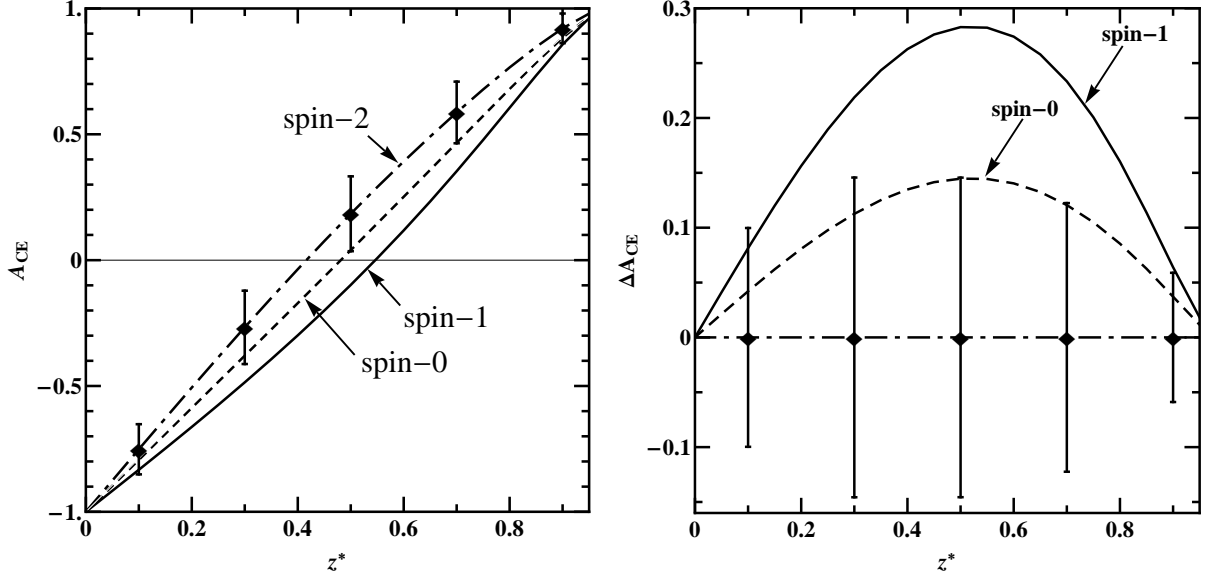


Figure 7: Left panel:  $A_{CE}$  vs.  $z^*$  for the spin-2 resonance  $G$  at  $c = 0.01$  and  $M_R = 1.6$  TeV (dot-dashed curve), and for the spin-0 (dashed curve) and spin-1 (solid curve) hypotheses, all for the same  $M_R$  and number of events. The error bar at  $z^* = 0.5$  is within the identification reach on  $G$  (at the  $2\sigma$  level) for  $\mathcal{L}_{\text{int}} = 100 \text{ fb}^{-1}$  as explained in the text. Right panel: Asymmetry deviations,  $\Delta A_{CE}$ , of the spin-1 and spin-0 hypotheses from the RS one, compared with the uncertainties on  $A_{CE}^G$ .

As an example, in Fig. 7 (left panel) the center-edge asymmetry  $A_{CE}$  is depicted as a function of  $z^*$  for resonances with different spins, same mass  $M_R = 1.6$  TeV and same number  $N_S$  of signal events under the peak. The dot-dashed curve corresponds to the spin-2 RS graviton with  $c = 0.01$ . The calculation is performed using the parton distributions mentioned in Sec. 2.2, and detector cuts as well as the SM background have been accounted for. Actually, the  $z^*$ -behavior of  $A_{CE}(z^*)$  resulting from the full calculation is found essentially equivalent to those presented in Eqs. (36)–(38). Differences are appreciable only for  $z^*$  close to 1, and turn out to have negligible impact on the numerical determinations of the identification reaches presented in the sequel, where the relevant chosen values of  $z^*$  are in a range around 0.5. Indeed, since numerically the  $\chi^2$  turns out to have a smooth dependence there, for definiteness we will present the results obtained from  $A_{CE}(z^* = 0.5)$ .

The deviations of the  $A_{CE}$  asymmetry from the prediction of the RS model, caused by the spin-0 exchange

$$\Delta A_{CE} = A_{CE}^G - A_{CE}^S \quad (39)$$

and that caused by the spin-1 exchange

$$\Delta A_{CE} = A_{CE}^G - A_{CE}^V, \quad (40)$$

respectively, are depicted in Fig. 7 (right panel). The identification potential depends, of course, from the available statistics (as well as on systematic uncertainties). In the example of Fig. 7, the vertical bars attached to the dot-dashed curve represent the  $2\sigma$  statistical uncertainty on the  $A_{CE}$  of the RS graviton model, assumed to be the “true” model consistent with the data as stated above, with the values of  $M_G$  and  $c$  reported in

the caption and integrated LHC luminosity of  $100 \text{ fb}^{-1}$ . One reads from Fig. 7 that, at such (high) luminosity, the spin-2 RS graviton with mass  $M_G = 1.6 \text{ TeV}$  and coupling  $c = 0.01$  can, indeed, be discriminated from the other spin-hypotheses by means of  $A_{\text{CE}}$  at  $z^* \simeq 0.5$ .

Actually, Eqs. (37) and (38) show the peculiar feature of  $A_{\text{CE}}(z^*)$ , that for same number of signal events:

$$A_{\text{CE}}^S(z^*) > A_{\text{CE}}^V(z^*), \quad (41)$$

for all values of  $0 < z^* < 1$ . This property is of course reproduced in Fig. 7, and allows to conclude that, in order to identify the spin-2 graviton resonance, if one is able to exclude the spin-0 hypothesis, the whole class of spin-1 models will then automatically be excluded, so that the spin-2 *identification* from the spin-1 hypothesis would be model-independent. Stated in a statistical language, Eq. (41) explicitly realizes the statement that discrimination of the spin-2 RS resonance from the spin-1 hypothesis requires, for a given confidence level, less events than the discrimination from the spin-0 one, as also noted in Ref. [4].

## 6.2 Numerical results for RS graviton identification

We now consider the determination of the spin-2 of the resonance, based on the assessment of the corresponding required minimal numbers of signal events under the peak,  $N_{\text{min}}$ . To this purpose, we consider the deviations of the (assumed to have been measured) center-edge asymmetry  $A_{\text{CE}}^G$  from those expected from pure spin-0 exchange,  $A_{\text{CE}}^S$ , and from spin-1 exchange,  $A_{\text{CE}}^V$ , defined by Eqs. (39) and (40), respectively.

Eqs. (36)–(38) continue being a useful representation of these matters and accordingly, before presenting results from full calculations, we write the deviation of Eq. (39) as follows:

$$\Delta A_{\text{CE}} = \epsilon_q^G A_{\text{CE},q}^G + \epsilon_g^G A_{\text{CE},g}^G - \epsilon_q^S A_{\text{CE}}^S. \quad (42)$$

In Eq. (42), the notations are:  $A_{\text{CE},q}^G \equiv 2z^{*5} + \frac{5}{2}z^*(1 - z^{*2}) - 1$ ;  $A_{\text{CE},g}^G \equiv \frac{1}{2}z^*(5 - z^{*4}) - 1$ ; and  $A_{\text{CE}}^S = 2z^* - 1$ . We reconsider the numerical example of Fig. 7, and note that around the chosen value  $z^* = 0.5$  the gluon fusion subprocess largely dominates the deviation of Eq. (42), due to  $A_{\text{CE},g}^G \gg A_{\text{CE},q}^G, A_{\text{CE}}^S$ . Actually, it is the only contribution at  $z^* = 0.5$ , because of the vanishing  $A_{\text{CE},q}^G = A_{\text{CE}}^S = 0$  at this point. This feature is found to hold more generally, also for the other values of  $M_G$  and  $c$  different from those in Fig. 7 or, in other words, this choice is optimal in the sense that  $A_{\text{CE}}$  shows maximal sensitivity to RS parameters there.

To get an “estimator” that determines the spin-2 parameter space where the spin-0 hypothesis could be excluded, the deviation (42) should be compared with the statistical uncertainty on  $A_{\text{CE}}$  expressed in terms of the desired number ( $k$ ) of standard deviations. We have the condition

$$|\Delta A_{\text{CE}}| = k \cdot \delta A_{\text{CE}}, \quad (43)$$

where, taking into account that numerically  $(A_{\text{CE}}^G)^2 \ll 1$  at  $z^* \simeq 0.5$ ,

$$\delta A_{\text{CE}} = \sqrt{\frac{1 - (A_{\text{CE}}^G)^2}{N_{\text{min}}}} \approx \sqrt{\frac{1}{N_{\text{min}}}}. \quad (44)$$

From Eqs. (43) and (44), one therefore obtains

$$N_{\text{min}} = N_{\text{min}}^S \approx \left( \frac{k}{\epsilon_g^G A_{\text{CE},g}^G} \right)^2. \quad (45)$$

Fig. 6 shows the contribution of gluon-gluon fusion to graviton production at the LHC as a function of  $M_G$ . One finds that, for  $c = 0.1$ , the SM background contribution is less than 1% for all values of  $M_G$  considered.<sup>2</sup> Extracting the value of  $\epsilon_g^G$  from Fig. 6, one can easily evaluate from Eq. (45) the minimal number of event samples required to exclude the spin-0 hypothesis (hence to establish the spin-2). For example, for  $M_G = 2$  TeV and  $c = 0.1$ , we would find that  $N_{\min}^S \simeq 38$  at the  $1\sigma$  level ( $k = 1$ ), compatible with results in Ref. [4]. The limiting number  $N_{\min}^S$  required for identification against spin-0 smoothly increases with  $M_G$  as  $\epsilon_g^G$  decreases, as shown in Fig. 6.

The behavior of  $N_{\min}^S$  *vs.*  $M_G$  is presented for  $c = 0.1$  in Fig. 8. It is derived from the full calculation including detector cuts, using the general Eq. (43), with  $k = \sqrt{3.84} = 1.96$ , corresponding to the exclusion of the spin-0 resonance at 95% C.L. The two solid lines in this figure represent the number of resonance signal events  $N_S$  *vs.*  $M_G$  at luminosities  $\mathcal{L}_{\text{int}} = 10 \text{ fb}^{-1}$  and  $100 \text{ fb}^{-1}$ , respectively. Their intersections with the line of  $N_{\min}^S$  *vs.*  $M_G$  determine the value of the graviton mass where the spin-0 hypothesis can be excluded. In this example,  $M_G = 2.4$  and  $3.2$  TeV at  $\mathcal{L}_{\text{int}} = 10$  and at  $100 \text{ fb}^{-1}$ , respectively. By repeating this procedure for all other allowed values of the parameter  $c$ , from 0.1 down to 0.01, one can determine the corresponding values of  $N_{\min}$  for excluding the spin-0 hypothesis and the related values of  $M_G$ . The result for  $N_{\min}$ , at integrated LHC luminosity of  $100 \text{ fb}^{-1}$ , is displayed in Fig. 9 as a function of graviton mass  $M_G$  (95% C.L.). The resulting domain defines the identification reach on the spin-2 of the resonance.

Quite similarly, one can separately estimate the minimal number of events required to discriminate the spin-2 from the spin-1 hypotheses, on the basis of the difference in Eq. (40). In the approximations adopted above for the spin-0 case, one would get the expression

$$N_{\min} \equiv N_{\min}^V \approx \left( \frac{k}{\epsilon_g^G A_{\text{CE},g}^G - A_{\text{CE}}^V} \right)^2. \quad (46)$$

From Eq. (46) and Fig. 6, the minimal number of spin-2 RS events needed for excluding the spin-1 hypothesis, and the relevant resonance masses  $M_G$  depending from the LHC luminosity, can be obtained. The example for  $c = 0.1$  is reported in Fig. 8.

The results of the full calculations of  $A_{\text{CE}}(M_R)$  including detector cuts, to determine the exclusions of the spin-1 and the spin-0 hypotheses in terms of the corresponding minimal number of events  $N_{\min}^V$  and  $N_{\min}^S$ , respectively, are presented for  $\mathcal{L}_{\text{int}} = 100 \text{ fb}^{-1}$  in Fig. 9. This figure is conceptually similar to Fig. 1. The combination of the spin-0 and spin-1 rejection domains determines a common exclusion area and thus the domain where the spin-2 of the RS graviton resonance can be established. This is the light gray domain labelled “Identification”.

Equivalent to the above procedure, the identification  $M_G$  and  $c$  can be assessed by means of a “conventional” (and simple minded)  $\chi^2$  criterion, where the  $\chi^2$  function is defined as:

$$\chi^2 = \left[ \frac{\Delta A_{\text{CE}}}{\delta A_{\text{CE}}} \right]^2, \quad (47)$$

with  $\Delta A_{\text{CE}}$  represented by Eqs. (39) and (40) to obtain the exclusion domains of the spin-0

---

<sup>2</sup>Conversely, the figure shows that, for  $c = 0.01$ , this background can be appreciably higher, see also Table 2.2, and should be taken into account.

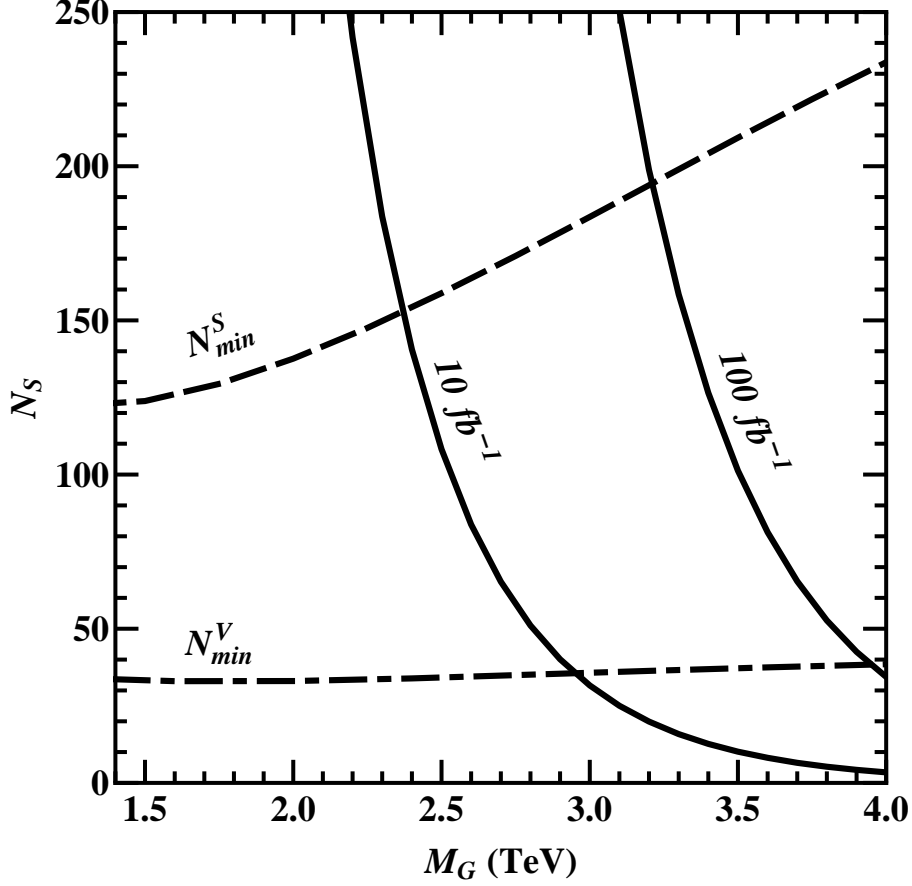


Figure 8: Minimal numbers of spin-2 events required to discriminate the spin-2 from the spin-0 ( $N_{\min}^S$ ) and spin-1 ( $N_{\min}^V$ ) hypotheses at 95% C.L. as a function of  $M_G$  at  $c = 0.1$ . The steep solid lines represent the number of spin-2 resonance (signal) events,  $N_S$ , which could be measured at the LHC at two chosen values of the luminosity,  $\mathcal{L}_{\text{int}} = 10 \text{ fb}^{-1}$  and  $100 \text{ fb}^{-1}$ , respectively.

and spin-1 hypotheses, respectively, and the statistical uncertainty

$$\delta A_{\text{CE}} = \sqrt{\frac{1 - (A_{\text{CE}}^G)^2}{\epsilon_l \mathcal{L}_{\text{int}} \sigma(G_{ll})}}. \quad (48)$$

Like before, the RS model can be assumed to be the “true” one, and the (95% C.L.) exclusion domains of spin-0 and spin-1 can be determined by requiring  $\chi^2 = 3.84$ , as pertinent to a one-parameter fit.<sup>3</sup> Like before, the maximal sensitivity of  $A_{\text{CE}}$  to the spin-2 RS resonance parameters is generally achieved for  $z^* = 0.5$ . Again, we combine the channels  $l = e, \mu$ . The 95% C.L. identification reach of the spin-2 hypothesis in the  $(M_G, c)$  plane then results from the domain complementary to the combination of the spin-0 and spin-1 exclusion domains. In fact, the spin-0 exclusion is more restrictive than that for spin-1, as discussed above.

---

<sup>3</sup>The parameters  $M_R$  and  $c$  are constrained via Eq. (13), rendering a two-parameter constraint effectively a one-parameter constraint.

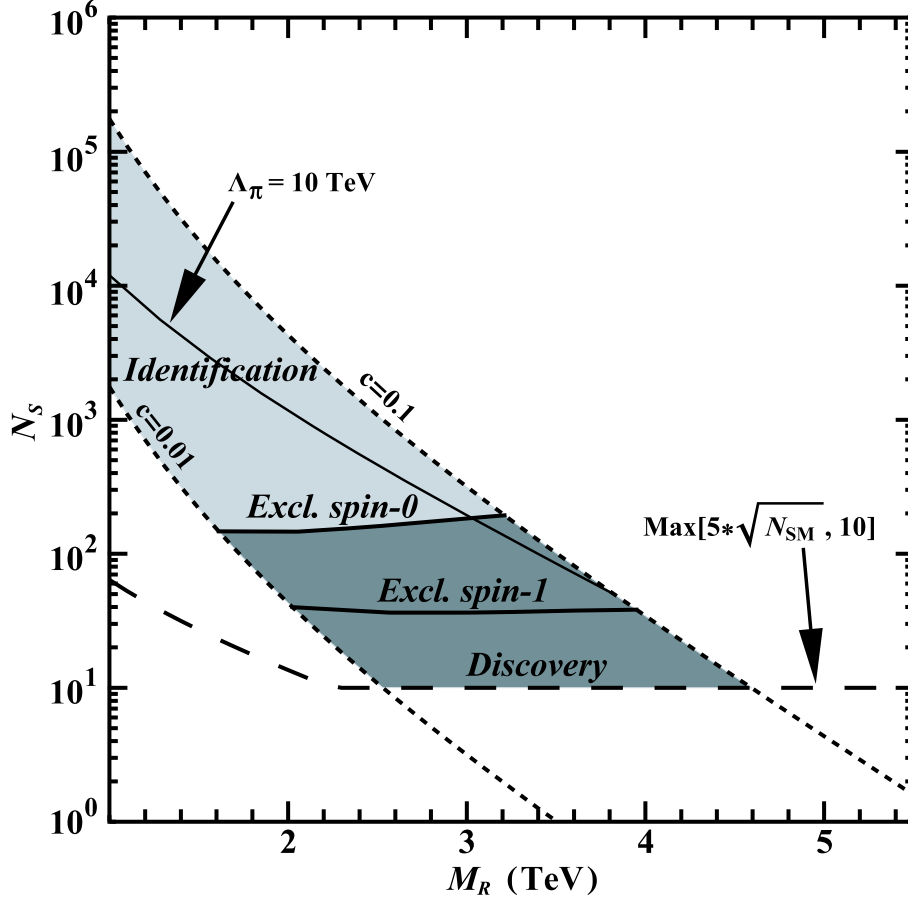


Figure 9: Same as in Fig. 1 but with exclusion limits and identification reach at 95% C.L. and  $\mathcal{L}_{\text{int}} = 100 \text{ fb}^{-1}$ . The channels  $l = e, \mu$  are combined. The theoretically favored region, limited by the  $\Lambda_\pi = 10 \text{ TeV}$  and  $c = 0.1$  lines, is also indicated.

## 7 Results in the RS parameter plane

The combined results of the previous section are presented, in the RS parameter plane  $(M_G, c)$ , in Figs. 10 and 11, for LHC integrated luminosities of  $10 \text{ fb}^{-1}$  and  $100 \text{ fb}^{-1}$ , respectively. The solid lines in these figures with attached labels “S” and “V” represent exclusion limits at the 95% C.L.

The dot-long-dashed line labelled as “ $G^{(1)}$ ” represents the  $5\sigma$  discovery reach on the lowest-lying RS graviton  $G \equiv G^{(1)}$  at each assumed luminosity. The resonance can be discovered if its representative point  $(M_G, c)$  lies to the left of this curve. Conversely,  $G$  could not be discovered if the corresponding representative point lies to the right.<sup>4</sup>

According to the discussion in Sec. 6.2, the domain to the left of the line labelled “V” represents the  $(M_G, c)$  values for which the spin-1 hypothesis for the first RS resonance can be excluded, but the spin-0 hypothesis is still left open. Finally, the domain to the left of the line labelled as “S”, represents the  $(M_G, c)$  values of the first RS resonance for which the alternative spin-0 hypothesis can be excluded. Reflecting the results in Sec. 6.2, this solid line lies to the left of the “V” one. Therefore, we may assume the combination of the

<sup>4</sup>Of course, all such statements must be understood in a statistical sense, as specified by the confidence level.

two respective domains shown as the shaded area, where both spin-1 and spin-0 hypotheses are excluded, to represent the lowest-lying RS resonance “identification” domain where the spin-2 character can be fully discriminated.<sup>5</sup>

Numerically, one can read from Fig. 10 that, for  $\mathcal{L}_{\text{int}} = 10 \text{ fb}^{-1}$  and the coupling  $c$  in the theoretically favored range, spin-1 can be excluded up to  $M_G = 1.3 \text{ TeV}$  for  $c = 0.01$ , and up to  $M_G = 2.9 \text{ TeV}$  at  $c = 0.1$ . Moreover, the spin-2 character of the resonance can be identified by spin-0 exclusion up to  $M_G = 1.0 \text{ TeV}$  for  $c = 0.01$  and up to  $M_G = 2.4 \text{ TeV}$  for  $c = 0.1$ . At the higher luminosity,  $\mathcal{L}_{\text{int}} = 100 \text{ fb}^{-1}$ , Fig. 11 indicates that the spin-1 hypothesis may be excluded up to  $M_G = 2.0 \text{ TeV}$  for  $c = 0.01$  and  $M_G = 4.0 \text{ TeV}$  for  $c = 0.1$ . The spin-2 of the RS resonance can be identified by spin-0 exclusion up to  $M_G = 1.6 \text{ TeV}$  for  $c = 0.01$  and  $M_G = 3.2 \text{ TeV}$  for  $c = 0.1$ .

Figs. 10 and 11 show rather clearly how the request of discriminating the spin-2 resonance from *both* the spin-1 and spin-0 hypotheses substantially reduces the “allowed” discovery domain in the  $(M_G, c)$  plane. Furthermore, this request reduces the size of the domain that would be allowed by the weaker condition of only discriminating spin-2 from the spin-1 hypothesis by a non-negligible amount. The theoretically “preferred” region, bounded from below (in  $c$ ) by the line  $\Lambda_\pi \lesssim 10 \text{ TeV}$  and also represented in these figures, is the source of a further, dramatical, restriction of the allowed region. However, this bound, rather than literally, should be considered as an order of magnitude indication. Also, the bound from the global fit to the oblique parameters, taken from Refs. [13, 37], has a qualitative character.

If producing more than one resonance is kinematically (and statistically) feasible, the fact that in the RS model the excitation spacing is proportional to the root of the  $J_1$  Bessel function also provides a signal for this scenario. It should therefore be important to examine the probability of observing the second excitation if the first resonance is discovered. Quantitatively, one should evaluate the cross section times the leptonic branching fraction for the DY production *via* the second excitation of the graviton state,  $G^{(2)}$ , as a function of the lowest-lying graviton mass  $M_G$ , and for the parameter  $c$  ranging from 0.1 down to 0.01. Neglecting interference between the two resonances, the result is that the  $n = 2$  graviton state  $G^{(2)}$  can be discovered at the LHC with  $10 \text{ fb}^{-1}$  of integrated luminosity, if the mass of the *lowest*-lying one  $G \equiv G^{(1)}$  is less than 1.1 TeV (2.7 TeV) at  $c = 0.01$  ( $c = 0.1$ ). With  $100 \text{ fb}^{-1}$ , discovery of  $G^{(2)}$  is possible if the mass  $M_G$  of the first excitation  $G^{(1)}$  is less than 1.6 TeV (3.7 TeV) at  $c = 0.01$  ( $c = 0.1$ ). All these numbers are at the  $5\sigma$  level. This clearly represents a significant discovery reach. The criterion to assess the discovery reach on  $G^{(2)}$  has been the same as for the discovery of  $G^{(1)}$ .

In Figs. 10 and 11, the line labelled as “ $G^{(2)}$ ”, represents the values of the first resonance mass  $M_G$  and  $c$  for which the second state,  $G^{(2)}$ , can also be discovered. In the  $(M_G, c)$  domain for  $G$  located to the right of that line,  $G^{(2)}$  could not be discovered. Conversely, for graviton  $G$  in the domain to the left of that line, the second graviton  $G^{(2)}$  can also be discovered. One can notice that in both figures this line is located between the “V” and the “S” lines, and this seems to be a general feature.

Therefore, taking into account the above discussion and the meaning of the various lines in Figs. 10 and 11, one can envisage the following possible scenarios in the discovery and identification of the lowest-lying RS resonance:

---

<sup>5</sup>Of course, barring other possibilities for the spin of the discovered resonance, not considered as basic starting point in our discussion.

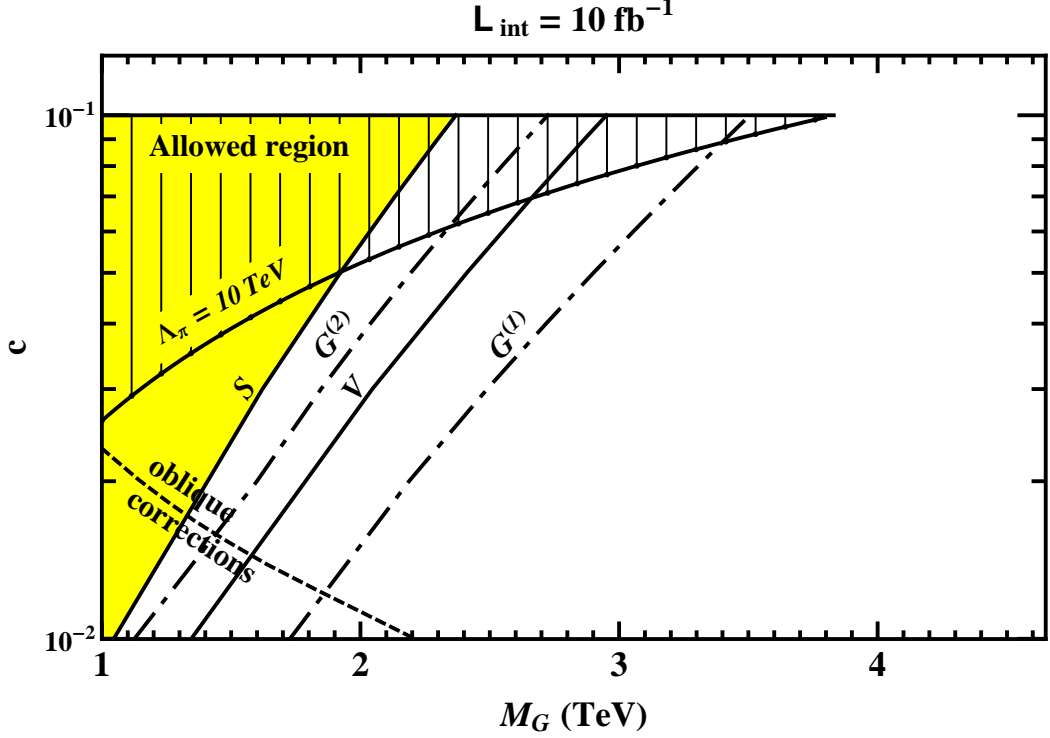


Figure 10: Discovery limits ( $G^{(1)}$  and  $G^{(2)}$ ,  $5\sigma$  level) and identification reaches ( $V$ ,  $S$ , 95% C.L.) on the spin-2 graviton parameters in the plane  $(M_G, c)$ , using the lepton pair production cross section and center-edge asymmetry, at the LHC with integrated luminosity of  $10 \text{ fb}^{-1}$ . The theoretically favored region,  $\Lambda_\pi < 10 \text{ TeV}$  (hatched), and bounds from the global fit to the oblique parameters, are also indicated.

- (i)  $G$  is discovered in the strip between the “ $V$ ” and “ $G^{(1)}$ ” lines, in which case only discovery of  $G$  is possible, but no identification;
- (ii) in the strip between the “ $G^{(2)}$ ” and the “ $V$ ” lines, where angular analysis can be used to exclude spin-1, but no spin-0 rejection and no production of the second resonance;
- (iii)  $G$  is found in the strip between the “ $S$ ” and the “ $G^{(2)}$ ” lines, in this case analysis based on the angular asymmetry  $A_{\text{CE}}$  can be performed to exclude spin-1, not spin-0 yet, but the second resonance  $G^{(2)}$  can be discovered and the RS spectrum test can be performed;<sup>6</sup>
- (iv) in the region to the left of the “ $S$ ” line indicated as the shaded area, the spin-2 character of the RS lowest-lying resonance can be identified and, in addition, the RS graviton mass spectrum can be verified by the discovery of the second resonance. Thus, the model would be doubly tested, by both the mass spectrum and the spin-2 angular analysis, and the RS resonance  $G$  clinched completely.

<sup>6</sup>In particular, as shown by Fig. 11, if one takes literally into account the severe bound  $\Lambda_\pi \leq 10 \text{ TeV}$ , at the high luminosity of  $100 \text{ fb}^{-1}$  such mass spectrum test should be operative in the full discovery region.

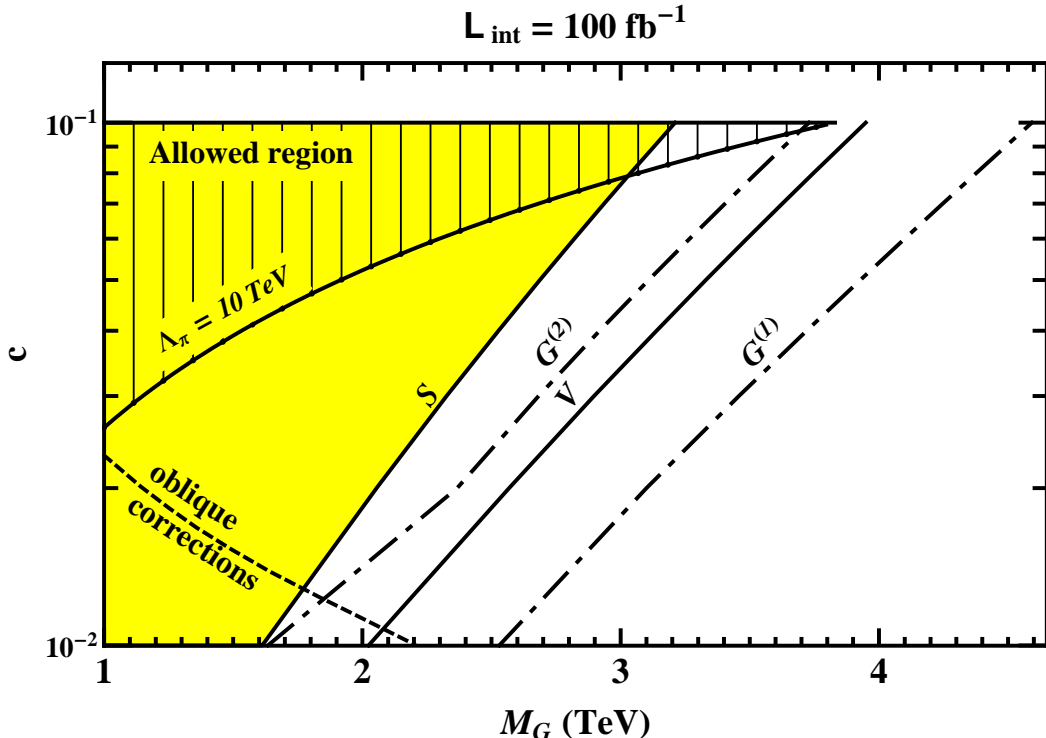


Figure 11: Same as in Fig. 10 but for the LHC integrated luminosity of  $100 \text{ fb}^{-1}$ .

## 8 Concluding remarks

In conclusion, we have considered the RS scenario, assuming a discovery can be made in the form of a resonance in the dilepton cross section. We have determined by an  $A_{\text{CE}}$ -based analysis up to what mass the spin-2 property can be established. This basically amounts to excluding the spin-0 hypothesis, in which case the spin-1 alternative will be automatically excluded. Additionally, we point out that in the parameter space where this spin determination is possible, the second resonance, with its characteristic mass, is also visible.

The analysis for the identification of the graviton spin can be performed using as basic observable the angular distribution of leptons itself, rather than the normalized angular-integrated center-edge asymmetry  $A_{\text{CE}}$ . Of course, one might expect that, with extremely high statistics, the two approaches could lead to equivalent results because, after all, the same data are used. However, if maintaining the same level of (high) statistics in each angular bin is required for the measurement of the differential cross section, an advantage of the method exposed here should be that a comparatively smaller event sample would be needed for the centre-edge asymmetry  $A_{\text{CE}}$  to obtain the constraints on the RS resonance at a given C.L. In addition, besides being “transparent” to spin-1 exchanges, the asymmetry  $A_{\text{CE}}$  might be less sensitive to systematic uncertainties (hence more sensitive to RS parameters) than an “absolute” angular distribution, because such uncertainties can be hoped to (at least partially) cancel.

The systematic uncertainties, not yet accounted for in the analysis presented above, originate from many sources, e.g., the accuracy of the theoretical calculations, the differences in the phenomenological determinations of the parton distribution functions, includ-



ing the uncertainties in the cross section predictions related to the choice of factorization scales as extensively discussed in Ref. [16], and the experimental uncertainties on the acceptance, electron identification efficiency, luminosity, and so on. Of course, the expectation is that these uncertainties should be mitigated by the basic observable  $A_{\text{CE}}$  being a ratio of (integrated) cross sections. The dominant experimental systematic error on the event rate can be expected to originate from the luminosity measurement, we conservatively assume at the 10% level, while uncertainties on efficiencies and acceptances should be at (or below) the 1% level [3]. Preliminary estimates seem to confirm the cancellation of such systematic uncertainties in  $A_{\text{CE}}$  alluded to before, and their almost negligible impact on the results for the identification reach on the spin-2 RS resonances presented in Sec. 7. We plan to investigate the effect of the other uncertainties mentioned above in a future analysis.

## Acknowledgements

This research has been partially supported by the Abdus Salam ICTP and the Belarusian Republican Foundation for Fundamental Research. AAP also acknowledges the support of MiUR (Italian Ministry of University and Research) and of Trieste University. The work of PO has been supported by The Research Council of Norway, and that of NP by funds of MiUR.

## References

- [1] L. Randall and R. Sundrum, Phys. Rev. Lett. **83** (1999) 3370 [arXiv:hep-ph/9905221]; *ibid.* Phys. Rev. Lett. **83** (1999) 4690 [arXiv:hep-th/9906064].
- [2] B. C. Allanach, K. Odagiri, M. A. Parker and B. R. Webber, JHEP **0009**, 019 (2000) [arXiv:hep-ph/0006114].
- [3] B. C. Allanach, K. Odagiri, M. J. Palmer, M. A. Parker, A. Sabetfakhri and B. R. Webber, JHEP **0212**, 039 (2002) [arXiv:hep-ph/0211205].
- [4] R. Cousins, J. Mumford, J. Tucker and V. Valuev, JHEP **0511**, 046 (2005).
- [5] I. Belotelov *et al.*, “Search for Randall-Sundrum graviton decay into muon pairs,” CERN-CMS-NOTE-2006-104.
- [6] D. Feldman, Z. Liu and P. Nath, JHEP **0611**, 007 (2006) [arXiv:hep-ph/0606294].
- [7] A. Abulencia *et al.* [CDF Collaboration], Phys. Rev. Lett. **95**, 252001 (2005) [arXiv:hep-ex/0507104].
- [8] E. W. Dvergsnes, P. Osland, A. A. Pankov and N. Paver, Phys. Rev. D **69**, 115001 (2004) [arXiv:hep-ph/0401199].
- [9] P. Osland, A. A. Pankov and N. Paver, Phys. Rev. D **68**, 015007 (2003) [arXiv:hep-ph/0304123].
- [10] J. Kalinowski, R. Ruckl, H. Spiesberger and P. M. Zerwas, Phys. Lett. B **406** (1997) 314 [arXiv:hep-ph/9703436]; *ibid.* Phys. Lett. B **414** (1997) 297 [arXiv:hep-ph/9708272];

- T. G. Rizzo, Phys. Rev. D **59** (1999) 113004 [arXiv:hep-ph/9811440];  
R. Barbier *et al.*, Phys. Rept. **420**, 1 (2005) [arXiv:hep-ph/0406039].
- [11] B. Allanach *et al.* [R parity Working Group Collaboration], arXiv:hep-ph/9906224.
- [12] For reviews see, *e.g.*: J. L. Hewett and T. G. Rizzo, Phys. Rept. **183** (1989) 193;  
A. Leike, Phys. Rept. **317** (1999) 143 [arXiv:hep-ph/9805494];  
P. Langacker, arXiv:0801.1345 [hep-ph].
- [13] H. Davoudiasl, J. L. Hewett and T. G. Rizzo, Phys. Rev. Lett. **84** (2000) 2080  
[arXiv:hep-ph/9909255]; *ibid.* Phys. Rev. D **63** (2001) 075004 [arXiv:hep-ph/0006041].
- [14] V. M. Abazov *et al.* [D0 Collaboration], Phys. Rev. Lett. **100**, 091802 (2008)  
[arXiv:0710.3338 [hep-ex]].
- [15] M. S. Carena, A. Daleo, B. A. Dobrescu and T. M. P. Tait, Phys. Rev. D **70**, 093009  
(2004) [arXiv:hep-ph/0408098].
- [16] P. Mathews, V. Ravindran, K. Sridhar and W. L. van Neerven, Nucl. Phys. B **713**,  
333 (2005) [arXiv:hep-ph/0411018]  
P. Mathews, V. Ravindran and K. Sridhar, JHEP **0510**, 031 (2005)  
[arXiv:hep-ph/0506158]  
P. Mathews and V. Ravindran, Nucl. Phys. B **753**, 1 (2006) [arXiv:hep-ph/0507250]  
M. C. Kumar, P. Mathews and V. Ravindran, Eur. Phys. J. C **49**, 599 (2007)  
[arXiv:hep-ph/0604135].
- [17] T. Han, J. D. Lykken and R. J. Zhang, Phys. Rev. D **59**, 105006 (1999)  
[arXiv:hep-ph/9811350].
- [18] G. F. Giudice, R. Rattazzi and J. D. Wells, Nucl. Phys. B **544**, 3 (1999)  
[arXiv:hep-ph/9811291].
- [19] J. Bijnens, P. Eerola, M. Maul, A. Mansson and T. Sjostrand, Phys. Lett. B **503**, 341  
(2001) [arXiv:hep-ph/0101316].
- [20] E. Dvergsnes, P. Osland and N. Ozturk, Phys. Rev. D **67**, 074003 (2003)  
[arXiv:hep-ph/0207221]  
T. Buanes, E. W. Dvergsnes and P. Osland, Eur. Phys. J. C **35**, 555 (2004)  
[arXiv:hep-ph/0403267].
- [21] R. Cousins, J. Mumford, V. Valuev, “Detection of  $Z'$  gauge bosons in the dimuon  
decay mode” in CMS, CMS Note 2005/002.
- [22] “ATLAS: Detector and physics performance technical design report. Volume 1,”  
CERN-LHCC-99-14  
“ATLAS detector and physics performance. Technical design report. Vol. 2,” CERN-  
LHCC-99-15
- [23] CMS Collaboration, “The CMS Physics Technical Design Report, Volume 1,”  
CERN/LHCC 2006-001 (2006). CMS TDR 8.1  
CMS Collaboration, “The CMS Physics Technical Design Report, Volume 2,”  
CERN/LHCC 2006-021 (2006). CMS TDR 8.2

- [24] J. Pumplin, D. R. Stump, J. Huston, H. L. Lai, P. Nadolsky and W. K. Tung, JHEP **0207**, 012 (2002) [arXiv:hep-ph/0201195].
- [25] D. Choudhury, R. M. Godbole and G. Polesello, JHEP **0208**, 004 (2002) [arXiv:hep-ph/0207248].
- [26] D. Choudhury, S. Majhi and V. Ravindran, Nucl. Phys. B **660**, 343 (2003) [arXiv:hep-ph/0207247].
- [27] For a review of experimental constraints on  $R$ -violating operators, see:  
G. Bhattacharyya, “A brief review of R-parity-violating couplings,” arXiv:hep-ph/9709395; Nucl. Phys. Proc. Suppl. **52A**, 83 (1997) [arXiv:hep-ph/9608415];  
H. K. Dreiner, arXiv:hep-ph/9707435, published in *Perspectives on Supersymmetry*, ed. by G. Kane, World Scientific;  
B. C. Allanach, A. Dedes and H. K. Dreiner, Phys. Rev. D **60**, 075014 (1999) [arXiv:hep-ph/9906209].
- [28] M. Cvetič and S. Godfrey, arXiv:hep-ph/9504216.
- [29] T. Aaltonen *et al.* [CDF Collaboration], Phys. Rev. Lett. **99**, 171802 (2007) [arXiv:0707.2524 [hep-ex]]; R. J. Hooper [D0 Collaboration], Int. J. Mod. Phys. A **20**, 3277 (2005).
- [30] A. A. Pankov and N. Paver, Phys. Rev. D **48**, 63 (1993).
- [31] See S. Riemann, in G. Weiglein *et al.* [LHC/LC Study Group], Phys. Rept. **426**, 47 (2006) [arXiv:hep-ph/0410364].
- [32] S. Godfrey, in *Proc. of the APS/DPF/DPB Summer Study on the Future of Particle Physics (Snowmass 2001)* ed. N. Graf, *In the Proceedings of APS / DPF / DPB Summer Study on the Future of Particle Physics (Snowmass 2001), Snowmass, Colorado, 30 Jun - 21 Jul 2001, pp P344* [arXiv:hep-ph/0201093].
- [33] M. Dittmar, A. S. Nicollérat and A. Djouadi, Phys. Lett. B **583**, 111 (2004) [arXiv:hep-ph/0307020].
- [34] T. G. Rizzo, arXiv:hep-ph/0610104.
- [35] F. Petriello and S. Quackenbush, Phys. Rev. D **77**, 115004 (2008) [arXiv:0801.4389 [hep-ph]].
- [36] A. Abulencia *et al.* [CDF Collaboration], Phys. Rev. Lett. **96**, 211801 (2006) [arXiv:hep-ex/0602045].
- [37] T. Han, D. Marfatia and R.-J. Zhang, Phys. Rev. D **62**, 125018 (2000) [arXiv:hep-ph/0001320].